UC Santa Barbara
UC Santa Barbara Previously Published Works

Title

Oxygen depletion and sediment respiration in ice-covered arctic lakes

Permalink

https://escholarship.org/uc/item/8cf8x2wx

Journal

Limnology and Oceanography, 68(7)

ISSN

Authors

Schwefel, Robert
MacIntyre, Sally
Cortés, Alicia
et al.

Publication Date

2023-07-01

DOI

Supplemental Material

https://escholarship.org/uc/item/8cf8x2wx#supplemental

Copyright Information

Peer reviewed

Oxygen depletion and sediment respiration in ice-covered arctic lakes

Robert Schwefel [1,2]* **Sally MacIntyre** [1,3,4] **Alicia Cortés** [3,5] **Steven Sadro** [3,6]
[1]Earth Research Institute, University of California at Santa Barbara, Santa Barbara, California
[2]Leibniz-Institute of Freshwater Ecology and Inland Fisheries–IGB, Berlin, Germany
[3]Marine Science Institute, University of California at Santa Barbara, Santa Barbara, California
[4]Department of Ecology, Evolution and Marine Biology, University of California at Santa Barbara, Santa Barbara, California
[5]Department of Civil and Environmental Engineering, University of California at Davis, Davis, California
[6]Department of Environmental Science and Policy, University of California at Davis, Davis, California

Abstract

Processes regulating the rate of oxygen depletion determine whether hypoxia occurs and the extent to which greenhouse gases accumulate in seasonally ice-covered lakes. Here, we investigate the oxygen budget of four arctic lakes using high-frequency data during two winters in three shallow lakes (9–13 m maximal depth) and four winters in 24 m deep main basin of Toolik Lake. Incubation experiments measured sediment metabolism. Volume-averaged oxygen depletion measured in situ was independent of water temperature and duration of the ice-covered period. Average rates were between 0.2 and 0.39 g O_2 m^{-2} d^{-1} in the shallow lakes and between 0.03 and 0.14 g O_2 m^{-2} d^{-1} in Toolik Lake, with higher rates in smaller lakes with their larger sediment area to volume ratio. Rates decreased to $\sim$ 20%–50% of initial values in late winter in the shallow lakes but less or not at all in Toolik. The lack of a decline in Toolik Lake points to continued oxygen transport to the sediment–water interface where oxygen consumption occurs. In all lakes, lower in situ oxygen depletion than in incubation measurements points toward increasing anoxia in the lower water column depressing loss rates. In Toolik, oxygen loss during early winter was less in years with minimal snow cover. Penetrative convection occurred, which could mix downwards oxygen produced by photosynthesis or excluded during ice formation. Estimates of these terms exceeded photosynthesis measured in sediment incubations. Modeling under ice-oxygen dynamics requires consideration of optical properties and biological and transport processes that modify oxygen concentrations and distributions.

During the long periods of ice-cover with low irradiance in arctic lakes, respiration is the dominant metabolic activity. Lakes become depleted in oxygen either near the sediments or in an appreciable part of the lake volume (Terzhevik et al. 2009; Kirillin et al. 2012). Fish habitats can be reduced or even complete fish kills can occur (Barica and Mathias 1979),

*Correspondence: robertschwefel@ucsb.edu

Additional Supporting Information may be found in the online version of this article.

and greenhouse gasses, phosphorus, and soluble reduced substances such as Fe^{2+}, Mn^{2+}, or NH_4^+ can accumulate (Karlsson et al. 2013; Denfeld et al. 2018; Jansen et al. 2021). Respiration in the sediments and at the sediment–water interface is largely responsible for oxygen depletion, and is described as sediment oxygen uptake (Terzhevik et al. 2010; MacIntyre et al. 2018; Bengtsson and Ali-Maher 2020). Overall depletion depends, in part, on the sediment surface area to volume ratio (Livingstone and Imboden 1996; Bengtsson and Ali-Maher 2020). This ratio then predicts, for lakes with similar benthic communities and sediment organic matter composition, higher loss rates in shallow ice-covered lakes (Leppi et al. 2016). However, comparative studies are rare which would identify other factors which determine temporal and spatial variability.

Processes that moderate metabolic rates and concentration of oxygen at the benthic boundary layer are likely sources of variability in rates of oxygen depletion under the ice. Water temperature determines rates of metabolic activity; hence, the cold water temperatures under the ice are expected to lead to reduced rates of respiration at the sediment–water interface

(Gudasz et al. 2010) and, for the typical range of temperatures under the ice, lower depletion rates when the water temperatures are colder (Golosov et al. 2007). Nevertheless, the influence of temperature is not completely understood. In a study of 15 mountain lakes, Smits et al. (2021) did not observe that oxygen depletion under the ice was dependent on temperature. However, their results were based on only one oxygen sensor in each lake. Metabolic activity and concomitant rates of oxygen depletion will also depend on the trophic state of the lake, with more rapid and greater depletion expected in the sediments of eutrophic lakes. Organic matter also flows into lakes from the watershed during the ice-free period, and the quantity of labile organic matter which settles to the sediments will also influence oxygen depletion over the winter.

Variations in oxygen concentration near the sediments will be moderated by the circulation under the ice. The predominant circulation, a form of horizontal convection, is induced by increases in density due to heat flux from the sediments and solutes produced by sediment respiration. It brings warmer water depleted in oxygen and enriched in the products of respiration to the deepest locations in lakes (Mortimer and Mackereth 1958; Malm 1998; MacIntyre et al. 2018). To balance the downward flow from the gravity currents, upward flow results away from the boundaries (Malm 1998). Thus, warmer water, although typically below 4°C, slightly enriched in solutes and depleted in oxygen, flows to the deep locations (Terzhevik et al. 2010; Pulkkanen and Salonen 2013). Over time, a density gradient can develop which is conducive to anoxia forming at the sediment–water interface (MacIntyre et al. 2018). The rate of downward flow depends on bottom slope, hence the set up for development of anoxia may depend on the ratio of surface area to depth. While the overall rate of oxygen depletion and thickness of the anoxic layer will depend on a lake's trophic status and supply of organic matter from the watershed, physical processes will moderate the oxygen gradient near the sediment–water interface and thus oxygen depletion rates.

Flux (F), and thus rate of oxygen depletion, depends on the oxygen gradient and physical processes. That is, $F = \delta/D$ $(C_s - C_w)$ where δ is thickness of the diffusive sublayer at the sediment–water interface, D is molecular diffusivity of the solute, and C_s and C_w are concentrations within the sediments and overlying water respectively (Wüest and Lorke 2003; Schwefel et al. 2017). As in studies at the air–water interface, δ depends on the extent of turbulence (MacIntyre et al. 1995; Lorke et al. 2003). Modeling has assumed both laminar and turbulent benthic boundary layers in ice-covered lakes (Malm 1998; Rizk et al. 2014) although evidence for turbulence is lacking. The water column often mixes or at least becomes weakly stratified prior to ice-on and oxygen concentrations are near saturation. Hence, the concentration gradient is likely to be high at the sediment–water interface following ice on when oxygen concentrations in the sediments are low. Processes that lead to its reduction will moderate the temporal changes in oxygen loss.

Oxygen depletion rates have been found to decline over the winter in the few studies with continuous time series data. This decline points towards either a thickening of the diffusive sublayer or a decrease in the oxygen gradient (Terzevik et al. 2009). Change in the thickness of the diffusive sublayer is expected to be less important than change in the oxygen gradient for the low levels of turbulence or the laminar flows expected under the ice (Schwefel et al. 2017). With the initially large concentration gradient at the sediment–water interface, there is considerable scope for it to decrease unless the water at the sediment–water interface is refreshed by more highly oxygenated water transported by gravity currents (Mortimer and Mackereth 1958; Terzhevik et al. 2009; MacIntyre et al. 2018) or internal waves (Kirillin et al. 2009, 2012; Petrov et al. 2006; Cortés and MacIntyre 2020). Penetrative convection may occur if sufficient light penetrates the ice. This process would potentially transport more highly oxygenated water downwards and also slow the build up of anoxia. With a decrease in these flows, a progressive increase in near-bottom anoxia is expected and a concomitant reduction in oxygen depletion.

The date of ice on and meteorological conditions during the period of ice formation may influence oxygen dynamics. If ice on is early enough, if the ice is clear black ice, and if wind sweeps any snow off the ice (Sturm and Liston 2003), light may penetrate, and induce radiatively driven convection, also known as penetrative convection. In this case, with water temperatures below the temperature of maximum density, solar radiation warming near-surface water would increase its density causing instability and mixing as has been observed in spring (Farmer 1975; Austin 2019; Bouffard et al. 2019; Austin et al. 2022). Any increases in oxygen below the ice, for instance oxygen excluded on formation of the ice (Scholander et al. 1953; Huang et al. 2021) or produced by photosynthesis as has been observed in spring or in temperate lakes when sufficient light penetrates through the ice (Jewson et al. 2009; Bramburger et al. 2022), could be mixed downwards to depths where it can be detected by sensors below the ice. Thus, while respiration is expected to dominate oxygen budgets under the ice in arctic lakes, increases in oxygen induced by exclusion from the ice or by photosynthesis in the water column or in the sediments could depress depletion rates following ice-on.

The goal of our study is to develop a predictive understanding of oxygen dynamics under the ice. To that end, we investigate variations in patterns of oxygen depletion through time in four oligotrophic, arctic lakes of differing morphometry to understand the underlying physical and biogeochemical mechanisms that moderate oxygen concentrations and, as appropriate, to identify the environmental factors moderating these mechanisms. We present oxygen, specific conductance (SC), and temperature measurements using multiyear data from under-ice moorings. We compute rates of oxygen depletion and their temporal variability during the course of the winter and between years. The in situ data are complemented

by measurements of benthic metabolic rates in incubations with sediments collected from the margin and the deep basin of each lake. We focus specifically on (1) the variability of oxygen depletion between years and lakes and its dependency on drivers including water temperature, duration of the ice-covered period, and lake morphometry; (2) the change and causes of change in oxygen depletion rates during the ice-covered period, (3) the impact of variable snow cover in fall on oxygen depletion. The results contribute to understanding the processes regulating oxygen depletion in winter and predicting oxygen budgets of ice-covered lakes in a changing environment.

Methods

Measurement site

We studied four oligotrophic, dimictic, kettle lakes located on the North Slope of the Brooks Range, Alaska. The lakes range from 1.7 to 150 ha with the 3 smallest lakes $\sim$ 10 m deep and the largest, Toolik, 24 m deep in the main basin (Table 1). Toolik is a multibasin kettle lake, E1 has a shallow side basin, and the other two lakes, N2 and E5, have only one basin. Lakes are ice-covered for 9–10 months per year and mix or partially mix after ice-off in late May or June and mix in fall. The lakes are described in Luecke et al. (2014). Nutrient enrichment experiments were conducted in N2 from 1985 until 1990 (O'Brien et al. 2005) and in E5 from 2001 until 2013 with results for benthic metabolism in summer in E5 described in Daniels et al. (2015). MacIntyre et al. (2018) illustrates thermal and density structure under the ice for Toolik and N2 and shows the more active horizontal convective circulation under the ice in the larger lake. They also predict the quantity of CO_2 produced under the ice for the full winter from the time series oxygen data and verified predictions with measurements. Cortés et al. (2017) and Cortés and MacIntyre (2020) describe the hydrodynamics and biogeochemistry of the lakes during winter with particular emphasis on snowmelt and mixing dynamics near ice-off. The focus in this article is on changes in oxygen in winter, defined as the period following ice-cover and before solar insolation increased in February.

Instrumentation

Time series measurements of temperature, oxygen, and conductivity were obtained with sensors on arrays at deep locations in each lake. The array in Toolik was in the larger Main Basin; an additional mooring was located in the side basin of E1. During summer, arrays cover the whole water column; in winter, the uppermost sensor is placed deeper than the expected maximal ice-cover. The design of the arrays used in the ice-free period is described in MacIntyre et al. (2009). The designs of the under-ice and in-ice moorings are described in Cortés et al. (2017) and Cortés and MacIntyre (2020). Overwintering and summer deployments always overlapped for a few days to assure continuity. Temperature was measured either with RBR

sensors (RBR 1050, 1060, or SoloT; 0.002°C accuracy, <10 s response time) or with Onset Water Temp Pros (0.2°C accuracy and 5 min response time). Calibrations of the RBR sensors were done yearly. The Onset Water Temp Pros were intercalibrated during periods of isothermy to enable 0.05°C accuracy. Sampling rates in the overwintering chains were between 5 and 900 s with shorter periods when RBR sensors were used with the sampling interval shortened in most cases after 2013/14. SC was measured using Onset U24-001 ($\pm$ 5 μs cm^{-1}) sensors with sampling rates of 1800 s. Dissolved oxygen (DO) was typically measured hourly with PME MiniDOT loggers ($\pm$ 0.3 mg L^{-1}). MiniDOTs were calibrated for conditions of no oxygen and 100% oxygen, and they and the SC loggers were intercalibrated, as needed, during periods of isothermy as typically occurred prior to ice on. Minimally six temperature loggers were deployed in each lake. At least three oxygen and conductivity loggers were deployed in the smaller lakes. Depths of the oxygen loggers in the water column are displayed in Fig. 1.

Oxygen depletion

Time series of DO on arrays were linearly interpolated as a function of depth. The resulting values were multiplied by the volume for each depth interval centered at the interpolation point using 1 m intervals. Total oxygen content was obtained by integrating from the bottom to 3 m below the ice surface. To assess the accuracy of calculations in $\sim$ 10 m deep E1, N2, and E5 with their 3–4 oxygen loggers (Fig. 1), oxygen concentrations were calculated using the full dataset from Toolik and then again from subsamples with three loggers (the uppermost, the deepest, and the third one from top; subsampling comparable to mooring designs used in the small lakes). The maximal difference was $\sim$ 3.2%. The main deviation occurs at the bottom of the water column which represents only $\sim$ 6% of the water column. This finding was consistent with comparisons between logger data and occasional hydrolab casts in the smaller lakes. Hence, we considered all calculated concentrations to be comparable when at least three loggers were used in the deployment.

Oxygen depletion was computed using two different approaches. The first, oxygen depletion rates in g O_2 m^{-2} d^{-1}, is based on the near-linearity of the decrease in oxygen concentration in early and late winter. The second, the decay rate with units per unit time, illustrates the changing rates over the winter with piece-wise exponential fits to the decreases in oxygen content. Early winter depletion rates were determined as linear fits of total oxygen depletion between ice-on and day of year (DOY) 300. DOY 300 was selected as depletion rates in the smaller lakes typically slowed by that date. Late winter depletion rates were fit between DOY 350 and 450 (DOY 85 of the following year). Fits were somewhat affected by internal wave motions which led to periodic changes of concentration below 2 m due to up- or downwelling of pycnoclines. Due to the slight nonlinearity especially in early winter, oxygen depletion rates must be considered as average values until DOY 300. The residuals often show an overestimation during
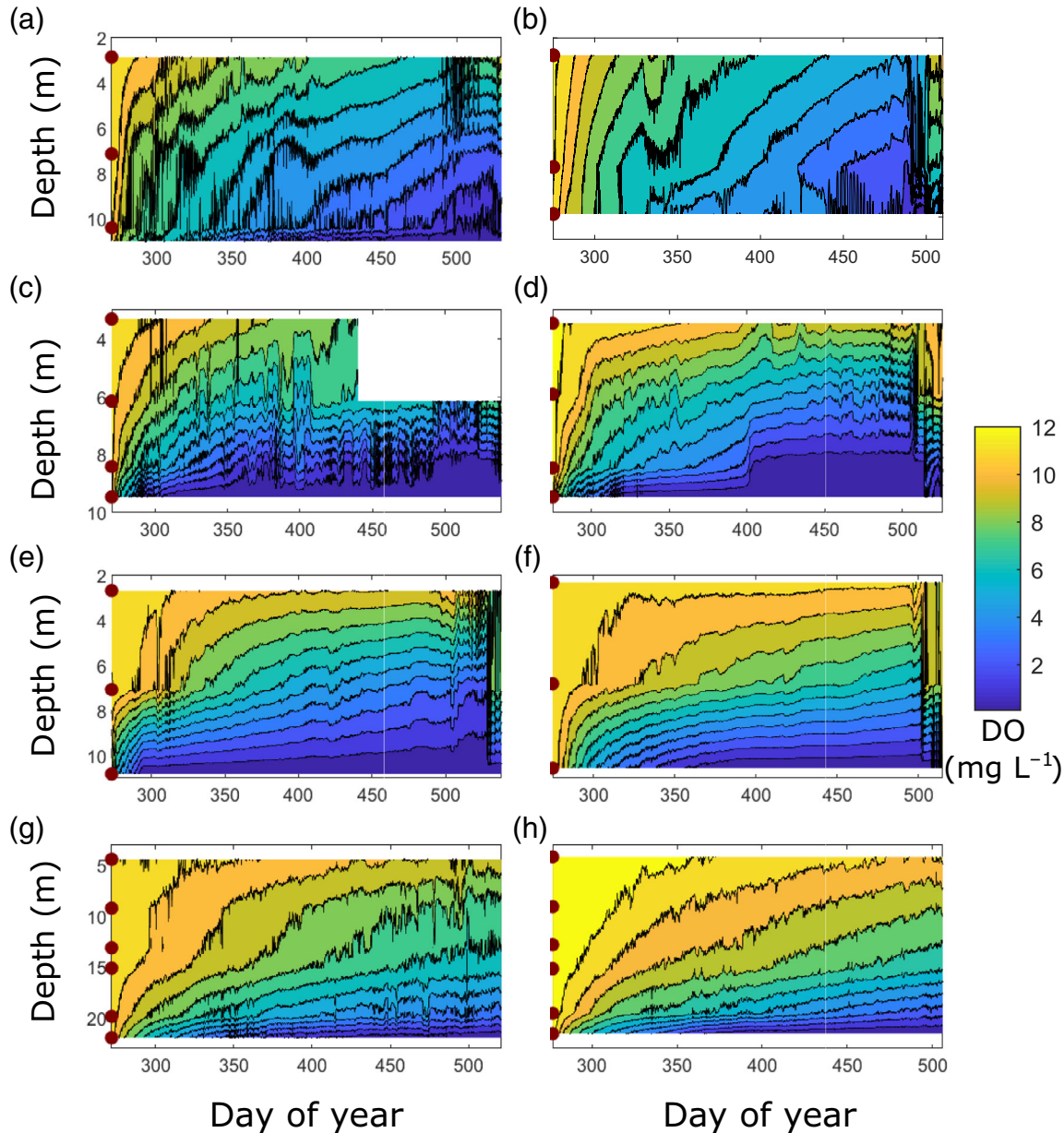
Table 1. Characteristics of the lakes (geographical location, depth, surface area, and volume), oxygen depletion rate (expressed as areal rate, volumetric rate, and total depletion over the whole winter) in early (ice on until DOY 300) and late winter (DOY 350–DOY 85 of the following year, i.e., 100 d), increase in SC in early and late winter (Rate SC, averaged over years in which data were available), ice on dates, and volume-averaged mean winter temperatures in E1, E5, N2, and Toolik.

Lake	Depth (mean/max) (m)	Surface area (ha)	Volume (1000 m³)	Oxygen depletion (mg O₂ m⁻² d⁻¹) (mg O₂ m⁻³ d⁻¹) (g O₂ m⁻³)‡ 13/14 Early winter	13/14 Late winter	14/15 Early winter	14/15 Late winter	15/16 Early winter	15/16 Late winter	17/18 Early winter	17/18 Late winter	Mean winter water temperature (°C) Ice-on date (DOY) 13/14	14/15	15/16	17/18	Rate SC (10⁻³ µs cm⁻¹ m⁻³ d⁻¹) Early winter	Late winter
E1 (68.626° N 149.555° E)	3.1/12	2.85	90	198	53	372	71	n.a.	n.a.	n.a.	n.a.	3.0 270	1.6 275	n.a.	n.a.	310*	165*
				64	17	120	23	n.a.	n.a.	n.a.	n.a.						
				6,3		7,9		n.a.		n.a.							
E5 (68.642° N 149.458° E)	6.3/13	10.86	691	369	82	286	63	n.a.	n.a.	n.a.	n.a.	2.0 273	1.1 276	n.a.	n.a.	n/a	n/a
				58	13	45	10	n.a.	n.a.	n.a.	n.a.						
				6.0		3.7		n.a.		n.a.							
N2 (68.640° N 149.626° E)	4.8/10.4	1.69	81	316	143	394	106	301	98	n.a.	n.a.	2.0 270	1.0 275	n.a.	n.a.	424 ± 75	249 ± 34
				66	30	83	22	63	21	n.a.	n.a.						
				n.a.		5.9		7.0		n.a.							
Toolik (main basin) (68.633° N 149.607° E)	7.0/26.3	94.01	6596	60	90	145	85	31	55	125	103	2.2 272	1.7 277	1.3 270	2.0 281	128 ± 55	96 ± 59
				8	13	21	12	4	8	18	14						
				3.1		3.2		2.6		3.2							

‡Computed until the date when values were least. Oxygen concentrations below 3 m no longer decreased after May.
*Only 1 yr of data available for the calculation.

Fig. 1. Contour plots of oxygen for Lakes E1 (**a,b**), N2 (**c,d**), E5 (**e,f**), and Toolik Lake (**g,h**) for the winters 2013/2014 (left column) and 2014/2015 (right column). DOY > 365 denotes the following year (e.g., DOY 366 in panel a refers to day 1 of the year 2014). Red dots indicate depths of the DO loggers. Isopycnals rise similarly to the oxygen isopleths except after ∼ DOY 300 in E1 and N2 where the downward progression of the cold surface layer precludes the rising of heat (data not shown).

the beginning and the end of the fitting period and an under-estimation in the middle. This pattern is indicative of an exponential decrease over the winter period quantified by the decay rate (see below). However, fits of the early and late winter period showed coefficients of determination (r^2) of mostly > 0.8 except for 1 yr at N2 (2013/14 late winter: $r^2 = 0.33$) and 1 yr in Toolik (2014/15 late winter $r^2 = 0.67$).

We obtained the decay rate (γ) by fitting an exponential curve to the data assuming oxygen depletion to be a first-order reaction (Terzhevik et al. 2010; Müller et al. 2012):

$$C(t) = C_0 e^{-\gamma t}. \tag{1}$$

Units are per unit time. Here, we present them as per year, with a value of $1 \, \text{yr}^{-1}$ indicating the initial value (C_0) decreases to $1/e \times C_0$ within 1 yr. Because γ was not constant, we used piecewise fits at 10-d intervals resulting in temporally varying values of γ. The change of γ over the course of the winter describes temporal dynamics of oxygen depletion and indicates the changes are not a first order reaction. The 10-d

interval exceeds the period of internal wave fluctuations insuring that fits were not effected by these motions.

Oxygen depletion co-occurs with solute fluxes from sediment respiration (Mortimer and Mackereth 1958). To quantify solute fluxes, volume-averaged SC was calculated using the same procedure as for volume-averaged oxygen concentrations. SC below 3 m was then linearly fit for early and late winter. The average increase (in $\mu s\,cm^{-1}\,m^{-3}\,d^{-1}$) was then converted to sediment fluxes ($\mu s\,cm^{-1}\,m^{-2}\,d$) by multiplying by the ratio of sediment surface area to water volume.

Incubation measurements

Sediment incubations were conducted in spring and fall during 2012–2014 on cores that were collected at depths representing marginal (shallow) and profundal (deep) locations (MacIntyre et al. 2018). The near-shore areas of these lakes are rocky, and cores were taken at locations away from the rocks. The cores in fall were typically taken in September, before ice-on, except those in 2013, which were obtained in November. The cores in spring were taken when the lake was ice covered and, similar to the ones from November, were obtained after drilling though the ice. Triplicate cores were obtained at each depth from within an ~ 10 m² area using a gravity corer equipped with 9.5 cm acrylic coring tubes. Cores were returned to the laboratory within 2 h of collection and allowed to rest at temperatures as measured above the bottom for 8–12 h prior to incubation in a water bath at the same temperature (Daniels et al. 2015). Briefly, ~ 20–25 cm deep sediment cores were incubated with 15–20 cm of overlying water. The overlying water in the initial core was carefully siphoned off, filtered through a 0.45 μm filter, and slowly returned to the coring tubes without disturbing the sediments. Cores were incubated in the dark and gently stirred with a magnetic stir bar to prevent gradients in DO from forming within the chambers. DO in each core was measured using a Hach optical oxygen sensor at 5-min intervals over the 2–5 h incubations.

In May 2013 and May 2014, photosynthesis vs. irradiance (*P* vs. *I*) experiments were subsequently conducted. Maximum photosynthetically available irradiance (PAR) was ~ 350 μmol photons $m^{-2}\,s^{-1}$. After the dark incubations, subsequent ones were conducted beginning with 20% irradiance (~ 70 μmol photons $m^{-2}\,s^{-1}$), followed by 37% irradiance (~ 130 μmol photons $m^{-2}\,s^{-1}$), and 70% irradiance (~ 250 μmol photons $m^{-2}\,s^{-1}$), until the final incubation at 100% (~ 350 μmol photons $m^{-2}\,s^{-1}$) irradiance. As incubations were carried out sequentially, the cumulative exposure to light increased with each subsequent light level, reaching a total of ~ 10 h after the start of the 20% irradiance treatment. Volumetric rates of net oxygen change corresponding to respiration (ER), or with light treatments net ecosystem production (NEP), were computed by fitting a linear model to DO concentrations within each chamber and converted to areal rates using the volume to surface area ratio for each chamber (Daniels et al. 2015). Gross ecosystem productivity (GEP) was computed from

measurements of ER and NEP using a simple mass balance model: GEP = NEP − ER, where rates of respiration were treated as negative values.

Results

The decline in oxygen concentrations over time following ice-on is evident in all the lakes, with more rapid loss in the two smallest lakes, N2 and E1 (Figs. 1 and S1). The depletion in oxygen can be seen at all depths with higher decreases in oxygen concentration at the bottom (Table S1). Isopleths of oxygen are continuously rising with progressively lower concentrations (Figs. 1 and S1). Rising isopleths are to be expected when gravity currents, induced by heat flux from the sediments and sediment respiration, flow to the bottom of a lake such that by continuity the overlying water rises (Mortimer and Mackereth 1958; MacIntyre et al. 2018). Thus, the rising isopleths result from the upward movement of water depleted in oxygen. Additionally, as near bottom density increases, intrusions may flow in above the bottom layer, contributing to the rapid rate of rise of oxygen isopleths. The rate of rise is higher in the two smallest lakes and progressively slower with the increase in lake surface area for E5 and Toolik. Periodic, relatively high frequency, fluctuations were anticorrelated with temperature and indicative of up- or down-welling movements of water due to internal waves (data not shown).

The lower water column often become anoxic (MacIntyre et al. 2018). The incidence and timing of anoxia are dependent not only on the oxygen depletion but also on how close the deepest sensor is to the bottom. In N2 and E5, anoxia developed within 50–100 d of ice on. Anoxia even developed in oligotrophic Toolik (Figs. 1 and S1). It was delayed in the main basin of E1 but developed quickly in the shallow side basin.

Mean winter water temperatures ranged from 2°C to 3°C in 2013/2014 and from 1°C to 1.7°C in 2014/2015 (Table 1). Temperatures were least in Toolik in 2015/2016. Temperature differences in the water column directly after ice-on, with the exception of Toolik, were greater when mean water temperatures were warmer.

Oxygen depletion rates across lakes

Volume-averaged concentrations in each lake following ice-on were ~ 12 mg $O_2\,L^{-1}$ (Fig. 2), close to saturation for the cold temperatures and altitude of these lakes (0.3–3.2°C in early winter and 745 m). Total oxygen depletion during winter was higher in the three small lakes relative to Toolik (Table 1), with some between year variability. The lowest value occurred in Toolik, 2.6 g $O_2\,m^{-3}$ in 2015/16, and the highest in E1, 7.9 g $O_2\,m^{-3}$ in 2014/15. Average areal rates varied by lake (Table 1). The lowest areal rates in early winter were measured in Toolik; the highest values were obtained in E5 and N2 (Table 1). Rates decreased nearly five-fold in late winter in
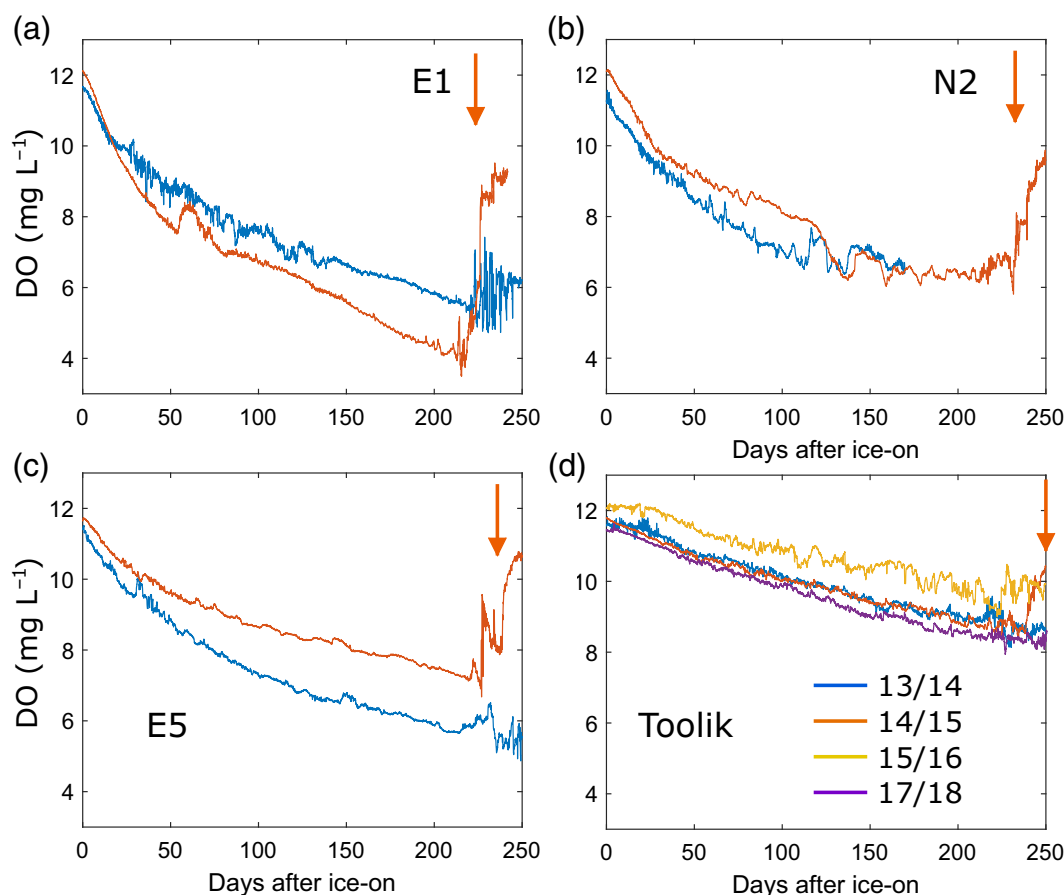
Fig. 2. Volume-averaged oxygen concentrations in Lakes E1 (panel a), N2 (panel b), E5 (panel c), and Toolik Lake (panel d) during the first 250 d after ice-on. The associated increase in SC is shown in Fig. S2. Arrows indicate ice-off in 2015. Oxygen starts to increase before ice-off as a result of incoming snowmelt (Cortés et al. 2017) and possibly oxygen production in spring.

E1, N2, and E5, and slightly increased or decreased in Toolik (Table 1). In situ areal depletion rates for all the lakes for the full winter averaged 111 ± 23 mg O_2 m^{-2} d^{-1}.

Volume averaged oxygen concentrations followed two patterns in Toolik Lake (Fig. 2d). Values in 2014–2015 and 2017–2018 decreased linearly following ice-on. In contrast, those in 2013–2014 and 2016–2016 were almost constant for about 30 d following ice-on. The time series data indicated that concentrations increased at the depths of the uppermost sensors in these 2 yr (Fig. S1).

SC increased as oxygen was depleted (Figs. 3a and S2). In early winter, the increases in SC and decreases in oxygen were highest in the two shallow lakes, N2 and E1. Both have higher concentrations of organic matter in the sediments than Toolik (MacIntyre et al. 2018). Increases in SC in Toolik were about half of those in the two small lakes in early winter and similar to those in the small lakes in late winter. The ratio of the average increase in SC to that of oxygen in early winter in the small lakes was ~ 12, whereas in late winter, it was ~ 9, indicating a greater production of solutes in the small lakes relative to oxygen loss in early winter relative to late winter. The ratio of SC increase to O_2 decrease was even higher in Toolik

Lake in early winter during the two winters in which initial rates of oxygen depletion were low (Table 1).

Changes in the decay rate

Temporal changes in the decay rate (γ; Eq. 1) were more pronounced in the three smaller lakes while γ was lower and in some years steadier in Toolik (Figs. 3b and 4a). γ was highest in E1, reaching 4 yr^{-1} in 2014/15 and then decreased rapidly within 2 months after ice on. Values in early winter were ~ 2.5 yr^{-1} in N2. Values were 2 yr^{-1} and nearly 3 yr^{-1} in E5 with the higher rate in 2013/14, the last year of the artificial fertilization of the lake. In Toolik, γ was relatively consistent in two of the winters (2014/15 and 2017/18); in the other two it was initially lower and increased within a few weeks of ice on (Fig. 4a). Time-lapse photographs of Toolik lake (https://www.uaf.edu/toolik/edc/monitoring/abiotic/time-lapse.php) confirmed that either snow-cover was absent or that it was patchy and lower than in the other years following ice-on, allowing light penetration, in the years with lower γ. In such years, oxygen concentrations at the depths of the uppermost sensors initially had increases in oxygen concentrations (Fig. 4b), and temperatures in the upper few meters
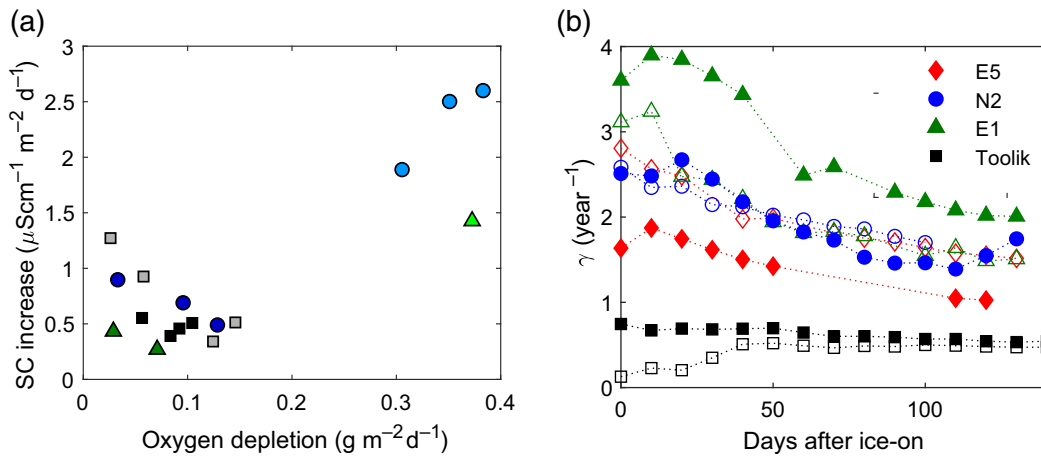
Fig. 3. (**a**) Rate of increase in specific conductance [SC] per unit area in E1 (2014/15; green triangles), N2 (2012/13, 2013/14, 2014/15; blue dots), and Toolik (2012/13, 2013/14, 2014/15, 2018/19; black squares) vs. areal oxygen depletion. Light colors refer to early winter, dark colors to late winter. E5 not included due to insufficient SC loggers. (**b**) Temporal change in the decay factor γ in Lakes E1 (green triangles), N2 (blue circles), E5 (red diamonds), and Toolik Lake (black squares) in years 2013/14 (open markers) and 2014/15 (filled markers). Data were fit to Eq. 1 over 10-d intervals.

increased in the day and then mixed with the underlying water, with the mixing indicative of penetrative convection (Fig. 4c). Fluctuations in oxygen concentration and in temperature increased near the bottom during the period with penetrative convection implying a downward propagation of energy. In years with persistent snow cover, temperatures in the upper water column increased more smoothly.

The daily change of heat in the water column after ice-on in 2015 estimates the amount of solar radiation penetrating through the ice as other contributors to the heat budget (e.g., sediment heat flux and heat loss at the ice-water interface) are small (Bengtsson and Svensson 1996). Values ranged from < 10 W m⁻² to 80 W m⁻² (Fig. S3). Comparison with the data of the meteorological station at the Toolik Field Station confirms that a considerable amount of incoming short wave radiation (up to 40%) penetrated the ice cover during days with low snow cover (Fig. S3). These calculations support our observations of radiatively driven convection
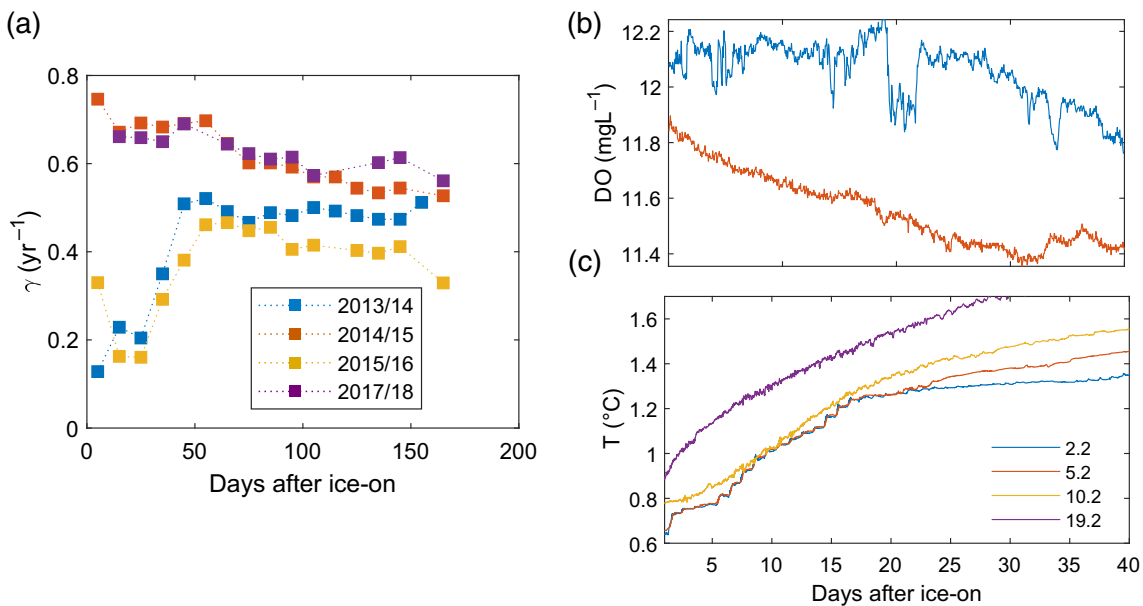
Fig. 4. (**a**) Temporal change in the decay factor γ in Toolik for four different winters. (**b**) Oxygen concentration at the uppermost logger in Toolik during winters 2015/16 at 6.6 m depth (blue, less snow cover), and 2014/15 at 3 m depth (red, higher snow cover). (**c**) Temperatures at 4 depths in 2015/16 illustrating the step-like increases in temperature and subsequent homogenization of temperature at 2.2 and 5.2 m and occasionally to 10.2 m, which began about 5 d after ice-on and persisted until 18 d after ice on, coinciding with the days with increased heating in the water column (Fig. S3). The homogenization is indicative of mixing events. In contrast, temperatures increased more smoothly in the upper water column in 2014/15 (data not shown).
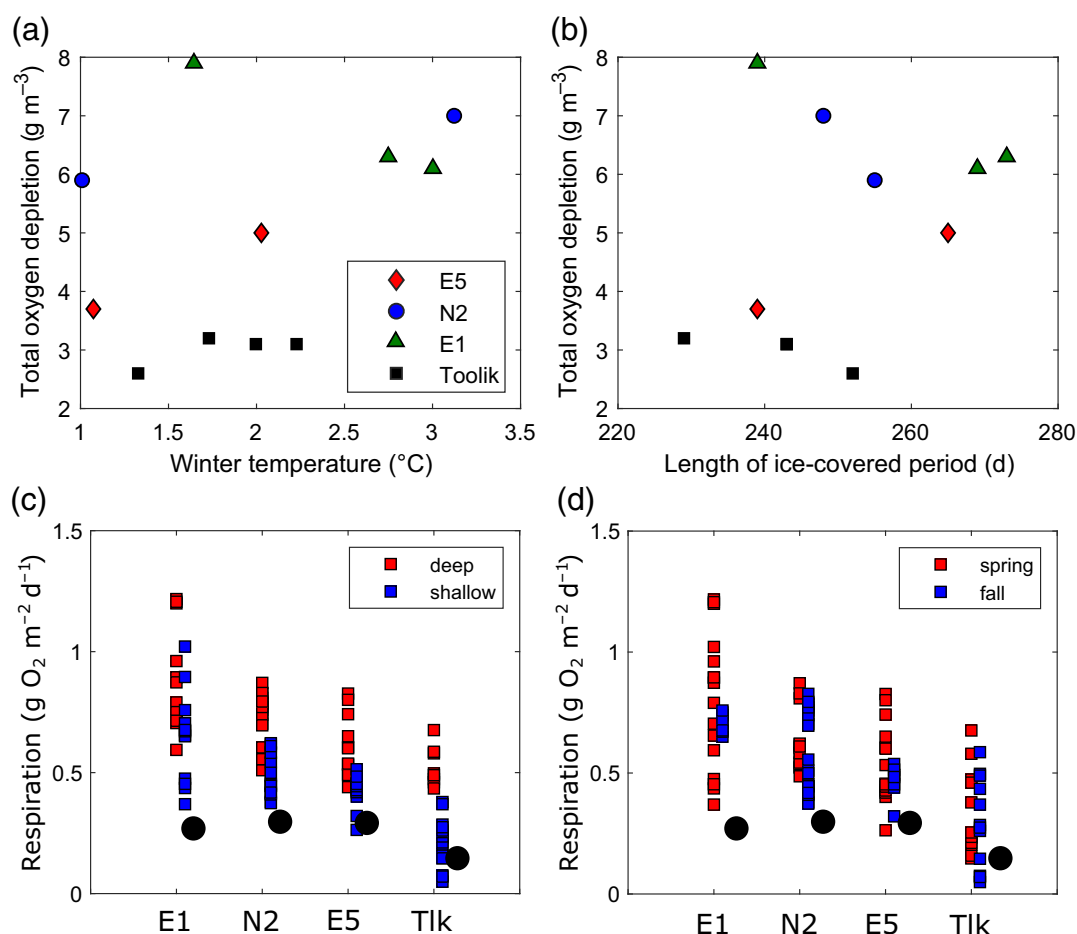
Fig. 5. (**a**) Total oxygen depletion based on oxygen change within the lakes as a function of water temperature in winter and (**b**) as a function of the length of the ice-covered period. (**c**) Respiration rates measured in incubations from samples taken in the shallow region and in the deep basin of E1, E5, and N2 and Toolik. The black dot indicates in situ oxygen depletion rates (in areal units) measured in early winter averaged over all years with data. (**d**) Same samples sorted by season.

occurring under the ice, which could moderate the distribution of oxygen.

Dependence of oxygen depletion on external factors

The decrease in oxygen was not statistically significantly correlated with the time between ice-on and the beginning of the convective period in spring (Pearson correlation coefficient $R = 0.33$, $p = 0.34$). Depletion rates were independent of mean water temperature during the winter period (Fig. 5a). Rates for early winter were also independent of temperatures near the bottom in early winter, and depletion rates were independent of mean lake temperature during the preceding summer (data not shown). There was no statistically significant correlation between total oxygen depletion and the duration of the ice-covered period ($R = 0.36$, $p = 0.27$; Fig. 5b). The correlation between early winter depletion and total depletion was very strong ($R = 0.88$, $p < 0.01$) while the one between late winter depletion and total depletion was weaker ($R = 0.65$, $p = 0.03$) indicating that early winter processes are

most relevant for winter oxygen depletion. Depletion in early winter depended on mean lake depth ($R = -0.89$, $p < 0.01$) while depletion in late winter was only weakly correlated with lake depth ($R = -0.37$, $p = 0.24$).

Respiration measurements

Respiration rates measured in experimental incubations in 2013 and 2014 (Fig. 5c,d and Table 1) were higher than the rates calculated from the in situ data. Rates were higher regardless of whether the calculation was based on the whole lake calculations or on the near bottom data, where the rate of oxygen depletion was higher (Table S1). Similar results were obtained in MacIntyre et al. (2018) only using the experimental data from autumn. Mean values ranged from ~ 0.9 g O_2 m^{-2} d^{-1} in the deep part of E1 to 0.2 g O_2 m^{-2} d^{-1} at the margin of Toolik, however, there was considerable variation by lake and by sampling depth. A multi-linear regression model with mean lake depth (mdepth), season (ssn; spring = −1; fall = 1), location of the sample (lcn; shallow region = −1; deep basin = 1), and year
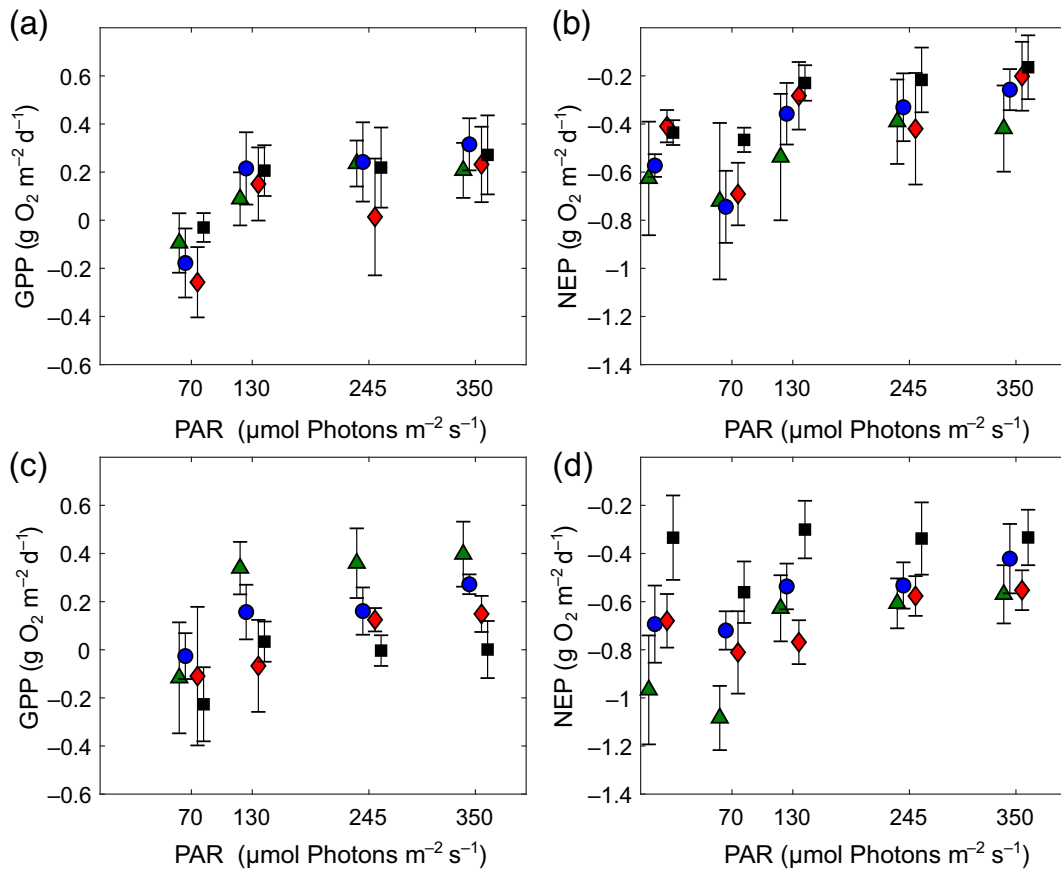
Fig. 6. Photosynthesis vs. irradiance curves (Photosynthetically available radiation, PAR μmol photons m^{-2} s^{-1}) from sediment core incubations in spring 2013 and 2014 in the shallow (**a,b**) and deep (**c,d**) sediments of Toolik Lake (black squares), Lake N2 (blue dots), Lake E1 (green triangles), and Lake E5 (red diamonds). Incubations measure NEP (panel b,d). Gross primary production (GPP mg O$_2$ m^{-2} d^{-1}, panel a,c) obtained by adding the NEP (panel b,d) values obtained in the dark (PAR = 0) to those obtained in the light. Points represent individual incubations aggregated across years for deep (top) and shallow (bottom) sites in each lake. Errorbars show the standard deviation of all measurements. Measurements were performed at 0 and $\sim$ 70, 130, 245, and 350 μmol photons m^{-2} s^{-1}, markers were shifted slightly to avoid overlap.

of measurement (year; 2013 or 2014) as independent variables explained 44% of variation in respiration rates ($R^2 = 0.44$). Allowing interactions between variables did not improve the model results ($R^2 = 0.48$), none of the interactions were statistically significant ($p > 0.1$ in all cases; data not shown). Only mean lake depth and location were identified as significant ($p < 0.0001$; Table S2). In general, respiration rates were higher in the deep basin of the lake and decreased as lake mean depth increased.

The proportion of oxygen depletion as measured in situ relative to those in the experimental incubations at shallow depths varied temporally. In situ rates of oxygen depletion in early winter were $\sim$ 75% of those obtained from the experimental incubations from shallow depths except in E1. They decreased to < 25% of respiration rates at shallow sites at E1, E5, and N2 by late winter. In Toolik, changes in depletion rates were less pronounced yet were still 50% of the values from the incubation measurements 100 d after ice-on.

Photosynthesis vs. irradiance experiments

Measures of gross and net production vs. irradiance had the expected shape of a photosynthesis vs. irradiance (P vs. I) curve for both shallow and deep sites (Fig. 6). Gross primary production (GPP) increased from negative values when there was no irradiance to positive values as irradiance approached or exceeded 70 μmol photons m^{-2} s^{-1} in the shallow cores, and NEP was negative at all irradiance levels but generally became less negative with increasing light (Fig. 6a,b). NEP tended to be more negative as irradiance initially increased. There are several mechanisms through which respiration may increase with light (Del Giorgio and Williams 2005), including increased heterotrophic activity associated with the release of dissolved organic matter (Sadro et al. 2011).

Our mass balance model assumed constant respiration at all light levels. Within the measurement accuracy, values of GPP at each irradiance were the same for each lake and values plateaued at $\sim$ 225 mg O$_2$ m^{-2} d^{-1}, with this value equivalent to P_{max}. I_k, the value of irradiance when the curve reaches

P_{max}, is between 70 and 130 μmol photons m^{-2} d^{-1}. We computed photosynthetic light efficiency (α) as the slope between 70 and 130 μmol photons m^{-2} s^{-1}. α was on average 0.054 $\pm$ 0.009 μg O$_2$ μmol photons^{-1} and showed no consistent trend.

For the deeper cores P_{max} was highest for E1, $\sim$400 mg O$_2$ m^{-2} d^{-1}, $\sim$150 mg O$_2$ m^{-2} d^{-1} for N2 and E5, and $\sim$ 75 mg O$_2$ m^{-2} d^{-1} for Toolik. These trends follow those for γ, particularly in early winter. I_k was in the same range for Toolik, N2, and E1, between 70 and 130 μmol photons m^{-2} d^{-1}, but was between 130 and 245 μmol photons m^{-2} d^{-1} for E5.

Discussion

Rates of oxygen depletion varied over the winter and by lake size. In the smallest lakes ($\sim$ 10 m and < 10 ha), initial rates were highest and then decayed. In the larger lake (24 m and 150 ha), rates were lower and tended to be more stable over the winter, or, in fact, even lower in early winter with a subsequent increase. The variability in rates of oxygen depletion and total oxygen depletion in the four lakes studied points to variable controls on oxygen dynamics. The greater depletion in the smaller lakes is to be expected based on the higher organic carbon content in their sediments (MacIntyre et al. 2018) and their greater sediment area to volume ratio (Bengtsson and Ali-Maher 2020). However, as will be seen in the following, other morphological features contribute. With the typically higher oxygen drawdown in early winter, oxygen depletion did not depend on the duration of the ice-covered period (Fig. 5b). Unlike Gudasz et al. (2010), who observed increases for temperatures from 1°C to 3°C in a eutrophic and an oligotrophic humic lake, we did not find a temperature dependence (Fig. 5a). Physical processes may have moderated the temporal dynamics in oxygen depletion to a greater extent than temperature as it moderated rates of metabolism. In the following, we evaluate the extent to which mean depth and the potential for water motion influence the patterns of oxygen drawdown in the smaller lakes relative to Toolik, the influence of basin morphometry on the depletion of oxygen in lakes of similar size, the importance of penetrative convection on depletion in Toolik in years with more or less snowcover, and we compare our results with those in other studies to provide further perspective on biological and optical controls on oxygen depletion under the ice.

Physical and biogeochemical controls on the time dependency of oxygen depletion in lakes of different size

Morphometry affects oxygen depletion in several ways. Observational and modeling data show that oxygen depletion during winter is primarily due to sediment oxygen demand (Terzhevik et al. 2010; MacIntyre et al. 2018; Bengtsson and Ali-Maher 2020). Higher depletion rates in shallow lakes are thus expected given their greater ratio of sediment surface area to lake volume and larger littoral area (Babin and Prepas 1985; Leppi et al. 2016; Bengtsson and Ali-Maher 2020). Benthic primary production during summer is highest in arctic lakes with shallower mean depths, implying more organic matter can be produced near the sediment–water interface in such lakes (Whalen et al. 2008). Thus, between lake differences in maximal rates of oxygen depletion in winter may go beyond the expected dependency on sediment surface area to lake volume by further depending on mean depth as it influences benthic production of organic matter in summer.

The decrease in oxygen depletion rates over the winter that we report has been observed in boreal lakes (Terzhevik et al. 2009, 2010; Bengtsson and Ali-Maher 2020) and alpine lakes (Smits et al. 2021). Terzhevik et al. (2010) attributed the higher rates of oxygen depletion to a turbulence-induced flux of water in a near bottom boundary layer to the overlying water, with calculated eddy diffusivities (K_z) two orders of magnitude higher than molecular rates (Petrov et al. 2006). With the reduction in the activity of seiches over the 2 months following ice-off, near-bottom flows are diminished (Petrov et al. 2006, 2007). Their study site, Lake Vendyurskoe, is a 5 m deep lake 10 km^2 in surface area, more susceptible to the action of wind on ice than our smaller, and in the case of all but Toolik, more sheltered lakes (Sturm and Liston 2003). Based on observations of internal waves and currents under the ice (Petrov et al. 2006, 2007), Terzhevik et al. (2010) argue that the deceleration of oxygen depletion from early to late winter resulted from a decrease in internal wave activity and associated near-bottom turbulence. Thus, similar changes in internal wave activity may influence the oxygenation of near-bottom waters and influence the decay rate (γ) in the lakes we studied.

The inference of reduced near bottom flow is supported by the analysis in MacIntyre et al. (2018), which includes calculations of the rate of rise of isopycnals over the winter in Toolik and N2 in 2013/14. While the rate of rise slows near the bottom in both lakes, the decrease is much faster in the smaller lake indicating a more rapid cessation of flow. The high frequency fluctuations of isopycnals of oxygen in Fig. 1 indicate that internal waves were present in all the lakes, although for a much shorter duration in L. E5. Internal waves are expected to have greater amplitude in large lakes for similar density stratification under the ice and similar wind speed acting to deflect the surface of the ice. Additionally, as the near surface boundary layer of cold water thickens, the depth over which stratification is weak is thinner in the smaller lakes (Cortés et al. 2017; Cortés and MacIntyre 2020), thus indicating internal waves would have smaller amplitude and would ventilate sediments over less of the water column in the small lakes. These combined factors indicate a larger area of the bottom may be influenced by internal wave motions and remain oxygenated in Toolik. However, the extent to which the horizontal convective circulation is sustained may be more critical. The more rapid upward rise of isopycnals in Toolik Lake than

N2 points to its longer continuation in Toolik (MacIntyre et al. 2018), and the greater production of solutes in the two small lakes (Fig. 4a) would induce a more rapid build up of near bottom density acting to suppress flow at depth in the smaller lakes. Thus, a combination of physical processes may have maintained the oxygen gradient for a longer period of time in the larger lake and limited reduction in γ whereas the rapid build up of near bottom density in the smaller lakes with accompanying anoxia may have led to the more rapid decay in γ.

A decrease in the abundance of reactive organic matter at the sediment–water interface could be another explanation for the decreasing rates in the smaller lakes. However, since oxygen depletion in the experimental incubations was similar in fall/winter and in spring (Fig. 5d), sediment oxygen demand probably did not change over the course of the winter. As fluxes of oxygen to the sediments depend on the gradient in oxygen (Bryant et al. 2010; Schwefel et al. 2017), we infer that a greater slowing of the convective circulation or a more rapid decline in any internal wave motions, and resultant decrease in the oxygen gradient, not changes in reactive organic matter, are the drivers of the more rapid decline in γ.

depletion rates in the smaller, shallower lakes relative to Toolik.

Physical and biogeochemical controls on the time dependency of oxygen depletion in small lakes of similar sizes

Complex morphometry may also influence oxygen depletion. For example, the western basin of E1 comprises about half of the surface area of the lake (Fig. 7a). The rates of oxygen depletion were higher in E1, with its side basin and extensive shallow areas, than in N2. Here, for lakes of nearly the same surface area and depth, mean depth would be a predictor variable for the overall extent of depletion. As was mentioned above and will be discussed further below, this difference may result from the greater benthic productivity in summer in lakes with shallower mean depths (Whalen et al. 2008) and subsequent respiration in winter (Karlsson et al. 2010). However, complex morphometry may contribute in other ways.

Complex morphometry may modify the flowpath of the horizontal convective circulation expected in small lakes. Near bottom waters of the shallow sidebasin of E1, at most 4 m deep, have a more rapid drawdown of oxygen than near-bottom
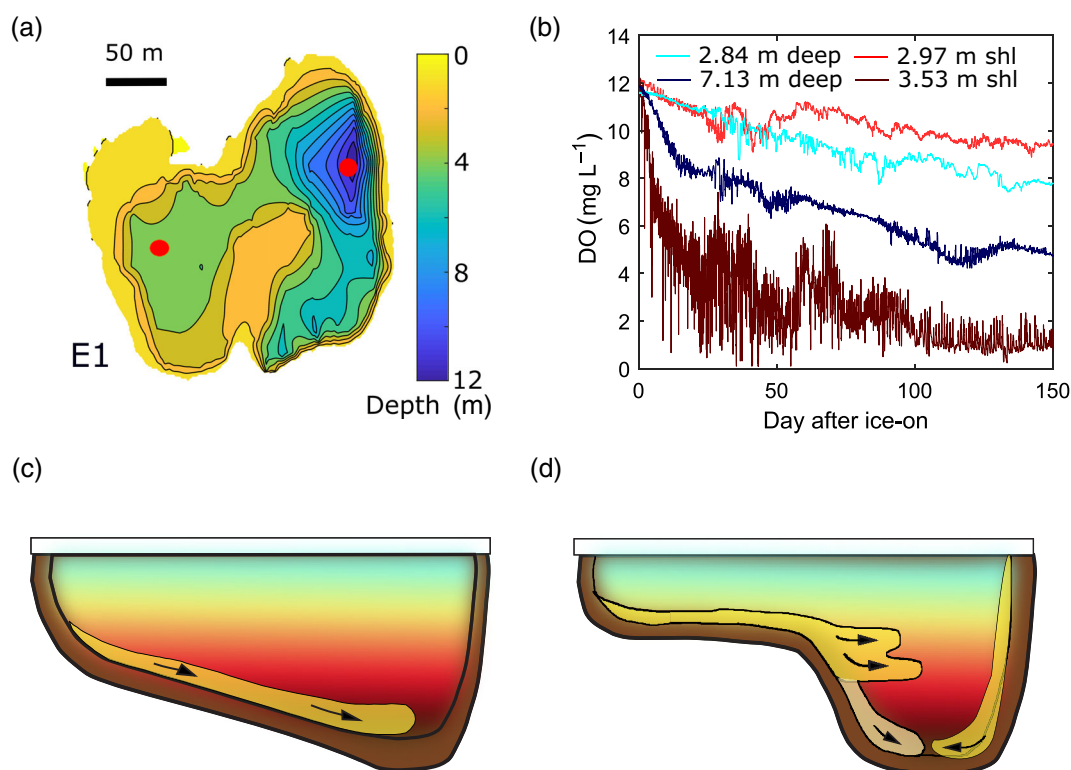

Fig. 7. (a) Bathymetry of E1 with the location of the two moorings as red dots. (b) Oxygen concentrations in the deep basin (deep) and in the shallow basin (shl) during winter 2013–2014. In the shallow basin, loggers were placed at 2.97 and 3.53 m depth, close to the sediments. The logger at 7.13 m in the deep basin is located at a depth with similar density as that at the bottom of the shallow basin. Hence, flow of water depleted in oxygen from the shallow basin would contribute to increased depletion rates in the main basin but not necessarily at the deepest depths. (c,d) Pathways of gravity currents in a lake with a simple bathmetry (c) and a lake with with an additional side-basin (d). In the latter, density-driven gravity currents or currents from wind-driven exchange may initially flow to the bottom (gravity current in dark brown) but, depending on the density near the bottom in the side basin relative to the main basin, could subsequently intrude mid-water column (gravity currents in yellow).

waters of the main basin (Figs. 7b and S1a). Near bottom temperatures in the side basin following ice on initially exceeded 4°C, implying a considerable increase in SC to maintain a stable water column. As the near bottom density increased in the side basin, overflows would have occurred from it and contributed to the overall oxygen decrease in the larger basin.

Appreciable fluctuations occurred in near-bottom oxygen at the shallow station. The largest decreases occurred as wind speeds peaked or changed direction, with values dropping below 2 mg L^{-1} at such times. As a result, not only density driven flows but also wind driven exchanges may have brought water from the western basin to the main basin. The water would flow to depths with similar density (Fig. 7c), whereas near-surface water of the side basin, with higher oxygen concentrations (Fig. 7b), would flow to shallower depths within the main basin. Thus, rather than downslope flows supplying the products of respiration initially to deep locations and then as density increases, to depths immediately above as expected for N2 and lakes with simple geometry (MacIntyre et al. 2018), the delayed flows from shallow embayments may lead to greater spatial and temporal variations of the flowpaths of water to the main basin (Fig. 7d).

Near-bottom oxygen concentrations within about a week of ice on varied from < 2 up to 6 mg L^{-1} in the side basin. As near bottom waters had higher SC and warmer temperatures, these variations are indicative of wind-driven tilting of isopycnals near the bottom and that bottom sediments were continuously being reexposed to oxygen. The refreshing of bottom water by the internal wave motions enables intermittent aerobic respiration in the side basin and subsequent more rapid drawdown of oxygen near the bottom. Such contrasts with the persistent anoxia near the bottom of N2 (Fig. S1b,c). These motions contribute to the overall greater oxygen depletion in E1 (Fig. 3b) and, with the inferred flows of water with lower oxygen concentrations offshore (Figs. 7b,d), the more rapid rise of oxygen isopleths in the main basin of E1 than in N2 (Fig. 1).

Methane dynamics may also be moderated by the additional flow paths and near-bottom oxygen drawdown in side basins of lakes with complex morphometry. CH$_4$ diffuses from the sediments and accumulates where the water is anoxic, typically at the bottom of the lake (Ducharme-Riel et al. 2015; Jansen et al. 2019). As anoxic water and any CH$_4$ produced in side basins flows to depths with similar density but replete with oxygen, methanotrophy may increase and convert the CH$_4$ to CO$_2$. Kettle lakes found in glaciated regions tend to have complex morphometry, hence mean depth and the presence of side basins may influence both oxygen depletion and the form of carbon.

Solar radiation, penetrative convection, and oxygen depletion

A striking difference between Toolik Lake and the smaller lakes was the low values of γ in early winter in Toolik in some years (Fig. 4a). While γ was initially elevated and consistently decreased in E1, N2, and E5 during all winters, it was around 0.4 yr^{-1} lower after ice-on in 2 yr at Toolik Lake and began to increase after ~ 30 d to values similar to those of the other years. The decrease corresponded to an ~ 0.08 g O$_2$ m^{-2} d^{-1} lower depletion rate in early winter during these years (0.05 g O$_2$ m^{-2} d^{-1} as opposed to 0.13 g O$_2$ m^{-2} d^{-1}). In the years with lower initial rates, examination of time-lapse photography of Toolik Lake showed that the lake surface more frequently had no snow cover or snow cover was at least reduced or only partial. Additionally, in such years, wind speeds were higher after ice-on, which can lead to snow being swept off the lake surface (Sturm and Liston 2003). Our time series temperature data indicated that penetrative convection, occurred in Toolik in early winter 2015 (Fig. 4c). Penetrative convection can then mix oxygen downwards assuming it has been increased near the surface by photosynthesis or when excluded as ice forms. In the following, we evaluate whether the lower oxygen depletion rates in years with minimal snow-cover was caused by oxygen production in the sediments (Fig. 6), photosynthesis within the water column as has been observed or inferred in spring or in temperate lakes (Hazuková et al. 2021; Hrycik and Stockwell 2021; Obertegger 2022), or exclusion of oxygen from the ice as it forms (Scholander et al. 1953; Belzile et al. 2001; Huang et al. 2021).

Photosynthesis in the sediments

We calculated production of oxygen in the sediments in g O$_2$ m^{-2} d^{-1} based on the incoming solar radiation at each depth assuming a diffuse attenuation coefficient of 0.6 (Cortés et al. 2017) (Fig. 8a,b), from the bathymetry of the lake (Fig. 8c), and the *P* vs. *I* curves measured in the sediment incubations (Fig. 6). I_k in our study was between 70 and 130 μmol photos m^{-2} s^{-1}, similar to values obtained in experiments with phytoplankton in summer (Evans et al. 2008), indicating that the benthic algae had been exposed to relatively high irradiance. In snow-free areas of the lake, incoming photosynthetically available radiation (PAR) exceeded 400 μmol photons m^{-2} s^{-1} (Fig. 8a) and thus even though our GPP measurements were conducted in spring, the benthic algae could similarly have acclimatized to higher irradiance in fall. However, even assuming an absolutely snow-free surface area, the additional oxygen production converted to the whole lake area in the first 30 d after ice-on was, on average, only equal to 0.004 g O$_2$ m^{-2} d^{-1} (maximally 0.014 g O$_2$ m^{-2} d^{-1}, Fig. 8d), on average 5% of the difference in oxygen depletion between years with high snow cover and years with low snow cover.

Primary production in the water column

Ice-on in the years with penetrative convection in Toolik Lake occurred in late September. While primary production was not measured under the ice, it was measured weekly for the first 3 weeks of September 2015 (Giblin and Kling 2022), stopping 1 week before ice-on. Integrated values for the upper 3 m, where primary production was highest, for these three
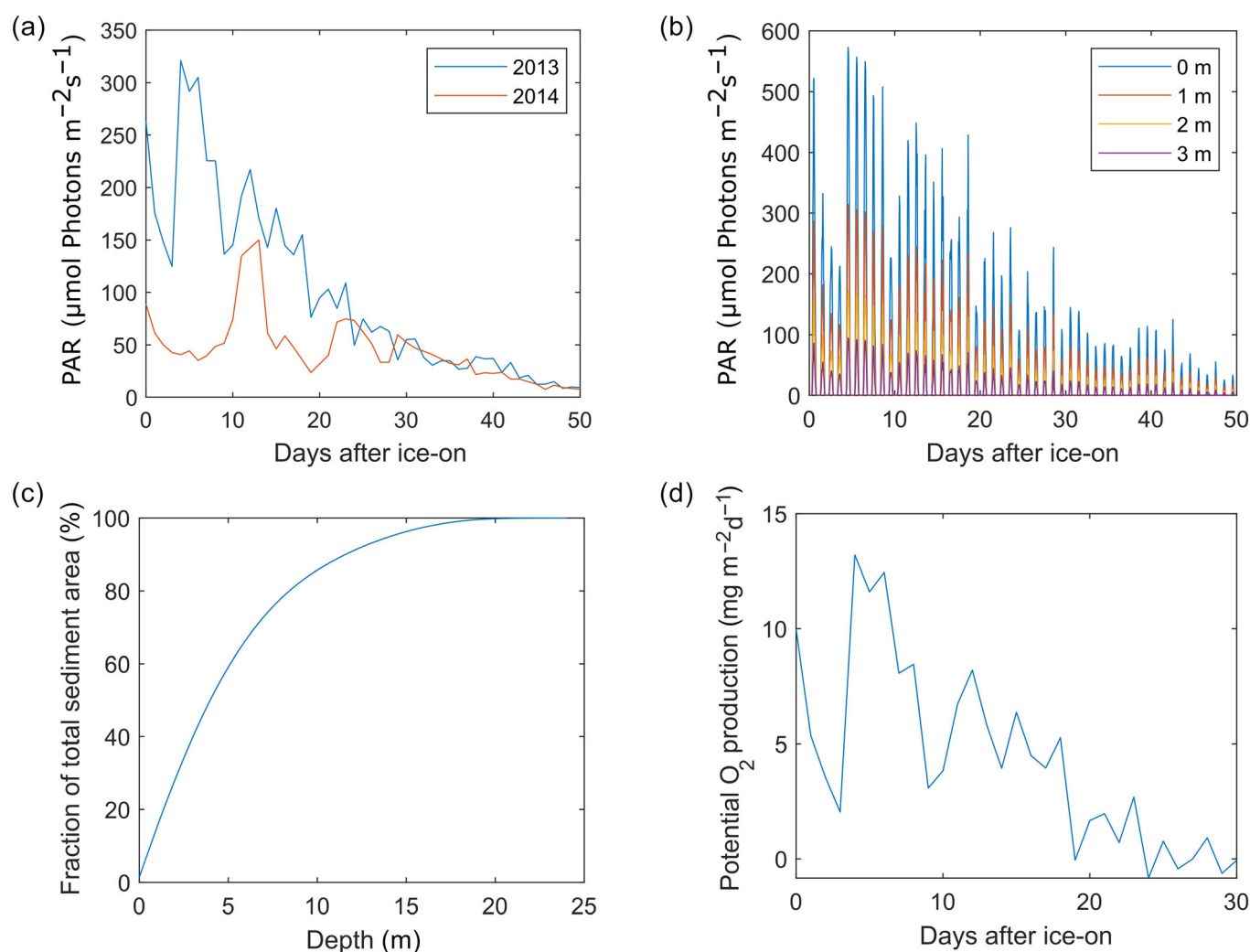
Fig. 8. (**a**) Incoming PAR (daily average during daytime) after ice-on in 2013 and 2014. (**b**) Hourly average of incoming PAR reaching 0, 1, 2, and 3 m depth in 2013 assuming an absence of snow cover and an attenuation coefficient of 0.6. (**c**) Cumulative sum of the sediment area of the main basin of Toolik Lake as a function of depth relative to the total sediment area. (**d**) Potential sediment oxygen production (daily average) in 2013 assuming incoming light as shown in panel b and $\alpha = 0.054$.

dates were 47.2, 55. 4, and 46.8 mg C m^{-2} d^{-1}, average chlorophyll a concentrations were 2 μg L^{-1}, and maxima of solar radiation on the sampling day and the following day, as incubations were over 24 h, were 488 and 481, 359 and 581, and 203 and 556 W m^{-2}, with considerable cloudiness on the 2 d with higher maximal irradiance.

Primary production can vary with temperature, irradiance, and phytoplankton abundance. However, Kremer et al. (2017) show that the changes in phytoplankton growth rates with temperature are least and negligible for some species at temperatures below 5°C. Whalen and Alexander (1986) (redrawn in Lizotte 2008) obtained areal photosynthesis in summer and winter in Toolik and found rates as the ice thinned in spring, water temperatures were 3°C, and chlorophyll a (Chl a) $\sim$ 2 μg L^{-1}, equivalent to mid-summer rates, 50 mg C m^{-2} d^{-1},

with these values similar to those in August 1999 in MacIntyre et al. (2006) (Chl $a \sim$ 1 μg L^{-1}) and in September in Giblin and Kling (2022). Based on the similarity of these estimates of primary production obtained at different water temperatures and relatively similar Chl a concentrations, primary productivity may not have have declined as water temperatures dropped following ice on.

Downwelling shortwave radiation during the period with penetrative convection reached up to 371 W m^{-2} with typical values $\sim$ 200 W m^{-2}, indicating a decrease in solar radiation from September into early October. Penetrative convection only occurred in the first 20 d after ice-on, and estimates of PAR to 3 m depth during this period (Fig. 8b) exceed the I_k values measured for phytoplankton in Toolik during the summer (Evans et al. 2008). While we cannot quantitatively assess the effects of

irradiance on primary production here, the experimental data in Evans et al. (2008) imply sufficient light to 3 m to enable growth. Assuming primary production under the black ice during early winter was similar to that in ice free conditions in September 2015, and also equivalent to that under 1 m of ice in spring (Lizotte (2008) recomputed from Whalen and Alexander (1986)), and irradiance was sufficient for growth for a third to a half of the days over which oxygen drawdown was reduced in early winter, the average oxygen production would be 0.04 to 0.07 g O_2 m^{-2} d^{-1}.

Density stratification develops quickly with ice on such that phytoplankton no longer circulate through the full water column, flagellates are predominant species in Toolik (Luecke et al. 2014), implying use of values of primary production based on bottle incubations would more accurately represent the metabolic rates during initial ice cover than those obtained during fall mixing.

Additionally, solute fluxes in early winters with penetrative convection are higher than in those without (Fig. 3a). Increases in solutes, such as bicarbonate, are attributed to sediment respiration (Mortimer and Mackereth 1958), however higher fluxes may point to penetrative convection increasing fluxes of solutes from porewaters at the depths to which the plumes descend (Hudson et al. 2022). The mixing may release reduced limiting nutrients which could also contribute to growth. These assessments indicate that oxygen produced by primary production and mixed downwards by penetrative convection could contribute appreciably to the difference in oxygen depletion in years with minimal to low snow cover in early winter vs. those with snowcover.

Exclusion of oxygen with ice formation

Due to the higher solubility of oxygen in liquid water compared to the ice phase, DO is excluded during the freezing process (Scholander et al. 1953; Belzile et al. 2001; Huang et al. 2021). Huang et al. (2021) measured oxygen concentrations of ice cores melted under vacuum and found oxygen concentrations to be 2–3 mg L^{-1}. Assuming that the amount of oxygen included in the ice is similar at Toolik Lake, and that the oxygen concentration of the water was initially 11–12 mg L^{-1} as measured before ice-on, ~9 mg L^{-1} oxygen would have been excluded from the ice during the freezing process. Ice thickness was measured approximately a month after ice-on and monthly thereafter with the monthly measurements indicating a near-linear increase in thickness for about 3 months. In 2013/14 and in 2015/16, the initial rate of increase was ~ 6 mm d^{-1} and 1 cm d^{-1}, respectively. If the upper water column is well mixed up to 10 m as in winter 2015/16, freezing would contribute 0.02–0.03 g O_2 m^{-2} d^{-1} to the oxygen budget below 3 m depth during early winter if the oxygen released is mixed downwards from the stable near-surface layer by penetrative convection (Fig. 4b,c). This increase corresponds to 25%–40% of the observed difference

in oxygen depletion between snow-free and snow-covered years in Toolik Lake. The more highly oxygenated water would be trapped within the stable surface layer if penetrative convection did not occur. Hence, exclusion of oxygen from the ice and subsequent downward mixing would explain a considerable fraction of the differences in oxygen depletion during years with and without penetrative convection.

Solutes are also excluded from the ice and would be mixed downward concomitantly with the oxygen. This process may have led to the larger increase in SC associated with low depletion rates in Toolik Lake (Fig. 3a). However, as the penetrative convection reached 10 m depth, the thermals may have induced flow near the sediments that may also have contributed to the increase in solutes. Thus, the increase in solute concentrations cannot definitely support oxygen exclusion as the mechanism leading to the lower oxygen depletion rates in years with lower snowcover following ice-on.

In summary, the oxygen deficit following ice-on in years with minimal snow cover was 0.08 g O_2 m^{-2} d^{-1} less than in years with snow cover. Primary production in the sediments can cause an increase of 0.004 g O_2 m^{-2} d^{-1}, and thus is a minor contribution to the deficit. However, the sediment cores on which this analysis is based sampled epipelic algae. The epilithic algae and the algae attached to the macrophytes found in between the rocks and visible to depths of at least 5 m could also contribute to oxygen production (Hecky and Hesslein 1995). The contribution from primary production is estimated to be in the range 0.04–0.07 g O_2 m^{-2} d^{-1}. Exclusion of oxygen from the ice and mixed downwards could account for 0.02 to 0.03 g O_2 m^{-2} d^{-1}. These results imply that a combination of oxygen exclusion from the ice and primary production could produce sufficient oxygen to account for the deficit in oxygen drawdown.

Comparisons with other studies
Oxygen depletion on a full lake basis

The averaged measured whole winter oxygen depletion for all the lakes, 111 ± 23 mg O_2 m^{-2} d^{-1}, corresponds, assuming a respiratory quotient of 1, to a carbon production rate of 42 ± 9 mg C m^{-2} d^{-1}. This value is similar to measured production of CO_2 in these lakes (MacIntyre et al. 2018) and in boreal lakes (Ducharme-Riel et al. 2015). The average depletion is less than reported in High Arctic L. Immerck (200 mg O_2 m^{-2} d^{-1}), which is 8 m deep with extensive littoral area such that the mean depth is 3.24 m (Michaud and Apollonio 2022). It is also less than reported from shallow prairie lakes (200 mg O_2 m^{-2} d^{-1}) (Barica and Mathias 1979), lakes in the upper mid-west of the U.S. (300 mg O_2 m^{-2} d^{-1}) (Ellis and Stefan 1989), and at the low end of the range (40–850 mg O_2 m^{-2} d^{-1}) reported for temperate, ice-covered lakes in Canada (Babin and Prepas 1985). Babin and Prepas (1985) determined that oxygen drawdown depended on mean depth and total phosphorus (TP) on an areal basis. Lakes in the Toolik region are phosphorus limited, with the range of TP for

lakes in this study 0.16–0.2 μM (Toolik, E1, N2) and 0.31 (E5) with the data from E5 including some years with the experimental fertilization (Luecke et al. 2014). The low average oxygen drawdown rates at our sites may in part be a result of low TP, which implies low pelagic primary production and the presence of iron oxide flocs, which would restrict P availability to some extent for benthic algae.

Values of γ at our study sites were comparable to these found in mesotrophic Lake Vendyurskoe in early winter (1.5–4.5 yr^{-1}, 0.5 to 1.5×10^{-7} s^{-1}) (Terzhevik et al. 2010; Zdorovennova et al. 2016). However, the values in the small lakes and Toolik exceeded those in L. Vendyurskoe in late winter (0.17–0.34 yr^{-1}). The anoxic layer in Lake Vendyurskoe was 1 m thick by the end of the winter, and variability in thickness of the anoxic layer and γ depended on the temperature at ice on; heat flux from the sediments, and organic matter accumulation. The combination of the lake's mesotrophy and shallow water column and large surface area likely led to a larger region with anoxia, which resulted in a lower γ in that lake in late winter.

Our results contrast with those of Bengtsson and Ali-Maher (2020) who did not observe differences in oxygen drawdown between years. This difference may be a result of the much larger volume of their study sites, Lakes Velen and Vendyurskoe, compared to the small lakes investigated in this study. It may also depend on morphological differences, such as mean depth, that can lead to more benthic production in some years. The differences in drawdown we observed in individual arctic lakes result from a suite of processes that moderate flow under the ice and which have a larger effect than small temperature differences.

Comparisons between estimates of GPP

Our estimates of GPP from our sediment incubations, once irradiance exceeded 70 μmol photons m^{-2} s^{-1}, were typically 100–200 mg O$_2$ m^{-2} d^{-1}. Photosynthetic rates of cyanobacterial mats in meltwater ponds characterized as undulating ice on the McMurdo Ice Sheet reached 640 mg O$_2$ m^{-2} d^{-1} during late summer (Vincent et al. 1993). GPP under the ice varied with depth in L. Hoare in the McMurdo Dry Valleys, with values in the upper 10 m ranging from near surface values of 370 mg O^2 m^{-2} d^{-1}, decreasing to 160 mg O^2 m^{-2} d^{-1} at 5 m, and increasing again to 290 mg O^2 m^{-2} d^{-1} at 8 m (Hawes and Schwarz 1999). The variations depended on algal concentrations and species composition. Given that the mats consist of algae and cyanobacteria, not sediments, it is not surprising that the values exceed what we obtained on an areal basis from sediment cores.

Comparisons between estimates of respiration

The differences between rates of respiration in our study with those in Gudasz et al. (2010) point to additional controls on sediment respiration during winter. The in situ rates of respiration we obtained in the shallow lakes, $\sim$ 0.25 g O$_2$ m^{-2} d^{-1}, (Fig. 5c,d) are similar to the values in Vallentunasjon (surface area 5.78 km^2 and depth 5 m), the eutrophic lake of Gudasz et al.'s (2010)

study, 0.2–0.3 g O$_2$ m^{-2} d^{-1} for temperatures below 5°C and assuming a respiratory quotient of 1. They are two and a half times higher than those in Svarttjarn (surface area 0.7 ha; maximum depth 6 m), the humic lake of Gudasz et al.'s (2010) study with organic matter derived from the landscape. The in situ rates in Toolik, 0.1 g O$_2$ m^{-2} s^{-1}, are equivalent to those in Svartttjarn. Rates from our experimental incubations, with methods similar to those in Gudasz et al. (2010), were even higher.

The low respiration rates in Svarttjarn relative to the shallow lakes in our study likely result from the higher dissolved organic carbon (DOC) within it, 28 mg L^{-1}, as opposed to 6 mg L^{-1} in the lakes near Toolik. Typically lakes with such high DOC in the boreal zone are highly stained and have high diffuse attenuation coefficients. Thus, they do not support abundant benthic algal communities as in lakes with clearer water (Ask et al. 2009; Seekell et al. 2015). Respiration in winter in shallow regions of clear lakes is supported by organic carbon from benthic algae (Karlsson et al. 2010). The lakes in the vicinity of Toolik have DOC concentrations of $\sim$ 6 mg L^{-1} (Kling et al. 2000), near the cut off between clear and dark northern lakes, 5 mg L^{-1} (Seekell et al. 2015), and have diffuse attenuation coefficients typically between 0.6 and 0.8 m^{-1}. Nearby lakes similar in depth to the three shallow lakes in this study supported benthic production which was $\sim$ 60% of primary production on a whole lake areal basis and for deeper lakes like Toolik, 40% to 75% of primary production (Whalen et al. 2008). Thus, the optical properties of the small lakes in this study enable growth of benthic algae, which can contribute to respiration in winter either by respiring themselves or by exuding organic matter.

The similarity of sediment respiration in the small lakes in this study, which are oligotrophic, to rates in eutrophic Vallentunasjon is surprising. Babin and Prepas (1985) predict that lakes with higher TP, and typically higher primary production and related settling of primary producers, will have higher winter respiration rates for the same mean depth. Here again, the differences in optical properties may be important. With the small lakes having clearer water than Vallentunasjon, production of benthic algae is supported. Thus, high algal biomass acts similarly to high concentrations of DOC in restricting light to the benthos, but lakes with higher algal biomass, and related higher attenuation coefficients, can support higher respiration rates in winter than lakes highly stained with DOC. As examples, benthic production explained the higher respiration rates in L. Immerck than expected for oligotrophic lakes in the High Arctic (Michaud and Apollonio 2022). Winter respiration in 6 m deep, 550 ha, subarctic Lake Almberga (average 160 mg O$_2$ m^{-2} d^{-1}, assuming a respiratory quotient of 1; DOC = 4 mg L^{-1}; TP = 0.38 μM) was similar to in situ oxygen drawdown in Toolik (Karlsson et al. 2008) and supported by benthic respiration at shallow depths and respiration of terrestrial organic matter at deeper depths. These comparisons point to the importance of optical properties of the water as it enables development and productivity of benthic communities in shallow regions in summer

(Daniels et al. 2015) and thus in regulating respiration rates in winter.

Thus, lakes with clearer water can have higher respiration rates in winter than lakes with considerably higher DOC and similar to lakes with high pelagic chlorophyll. Loading from the landscape also contributes. Benthic algae can continue to grow under the ice if there is sufficient light (Fig. 6a,c), and can continue to respire for some period under the ice. Benthic algae also exude organic carbon, the dominant energy source for respiration by heterotrophs at shallow locations under the ice (Karlsson et al. 2010). For example, the highest respiration rates in the experimental incubations at both the deep and shallow sites in our study were obtained in E1. The deep location in that lake is near the mouth of an incoming stream. Its mean depth is the least in the study, pointing to the importance of benthic production at shallow depths in the ice-free season followed by respiration of organic carbon produced by benthic algae during the ice-covered period. These comparisons indicate that oxygen drawdown, while it depends in part on the ratio of sediment area to volume and on loading from the landscape, is also highly dependent on optical properties of the water as they moderate benthic productivity.

Conclusions

Our between lake comparisons illustrate the importance of lake morphometry and ambient meteorology on oxygen drawdown during winter in arctic lakes. While the expected greater oxygen depletion occurred in shallow lakes, between year differences indicate additional physical and biological processes that can moderate depletion. Radiatively driven convection occurs following ice-on when snowcover is reduced and, with the downward mixing of water enriched in oxygen from photosynthesis and/or excluded during ice formation, oxygen depletion rates are lower. These observations point to the need for additional study of penetrative convection following ice-on and its implications for photosynthesis, near bottom mixing, and the onset of anoxia. Changes in precipitation as they influence snowcover have to be taken into account for an accurate prediction of future oxygen depletion rates under ice. Gross primary production increased in the sediments with increasing light. These increases only made a minor contribution to initially lower oxygen depletion rates in years with minimal snow cover. However, these data indicate a viable community of benthic algae was present that can release organic carbon that is respired by other microbes. They also indicate that as irradiance increases in spring, photosynthesis by benthic algae could consume some of the CO_2 produced over the winter. The presence of extensive shallow areas can lead to increased biomass of algae and other microbes during summer, which contribute to greater oxygen drawdown, as illustrated here, and production of greenhouse gases over the winter (Karlsson et al. 2008). Variations in lake morphometry and resultant differential rates of temperature increase, drawdown of oxygen, and solute production can also modify the expected flowpaths of gravity currents under the ice. The oxygen drawdown of the deeper basins can be enhanced, and the flow of solutes from sidebasins can spur microbial activity in the main basin which influences budgets of dissolved gases such as methane. Our observations contrast with earlier studies indicating that water temperature and duration of ice cover would be key determinants of overall drawdown of oxygen. They point to the need for additional studies following ice-on with emphasis on the contributions of shallow regions to respiration and the unexplored consequences of radiatively driven convection in early winter on photosynthesis and on the magnitude of flows and resultant biogeochemical and microbial processes at the sediment–water interface.

References

Ask, J., J. Karlsson, L. Persson, P. Ask, P. Byström, and M. Jansson. 2009. Terrestrial organic matter and light penetration: Effects on bacterial and primary production in lakes. Limnol. Oceanogr. **54**: 2034–2040. doi:10.4319/lo.2009.54.6.2034

Austin, J. A. 2019. Observations of radiatively driven convection in a deep lake. Limnol. Oceanogr. **64**: 2152–2160.

Austin, J., C. Hill, J. Fredrickson, G. Weber, and K. Weiss. 2022. Characterizing temporal and spatial scales of radiatively driven convection in a deep, ice-free lake. Limnol. Oceanogr **67**: 2296–2308.

Babin, J., and E. E. Prepas. 1985. Modelling winter oxygen depletion rates in ice-covered temperate Zone Lakes in Canada. Can. J. Fish. Aquat. Sci. **42**: 239–249. doi:10.1139/f85-031

Barica, J., and J. A. Mathias. 1979. Oxygen depletion and winterkill risk in small prairie lakes under extended ice cover. J. Fish. Res. Board Can. **36**: 980–986. doi:10.1139/f79-136

Belzile, C., W. F. Vincent, J. A. Gibson, and P. V. Hove. 2001. Bio-optical characteristics of the snow, ice, and water column of a perennially ice-covered lake in the high Arctic. Can. J. Fish. Aquat. Sci. **58**: 2405–2418. doi:10.1139/f01-187

Bengtsson, L., and T. Svensson. 1996. Thermal regime of ice covered Swedish Lakes. Hydrol. Res. **27**: 39–56.

Bengtsson, L., and O. Ali-Maher. 2020. The dependence of the consumption of dissolved oxygen on lake morphology in ice covered lakes. Hydrol. Res. **51**: 381–391. doi:10.2166/nh.2020.150

Bouffard, D., and others. 2019. Under-ice convection dynamics in a boreal lake. Inland Waters **0**: 1–20. doi:10.1080/20442041.2018.1533356

Bramburger, A. J., T. Ozersky, G. M. Silsbe, C. J. Crawford, L. G. Olmanson, and K. Shchapov. 2022. The not-so-dead of winter: Underwater light climate and primary

productivity under snow and ice cover in Inland Lakes. Inland Waters: 1–19. doi:10.1080/20442041.2022.2102870

Bryant, L. D., C. Lorrai, D. McGinnis, A. Brand, A. Wüest, and J. C. Little. 2010. Variable sediment oxygen uptake in response to dynamic forcing. Limnol. Oceanogr. **55**: 950–964. doi:10.4319/lo.2009.55.2.0950

Cortés, A., S. MacIntyre, and S. Sadro. 2017. Flowpath and retention of snowmelt in an ice-covered arctic lake. Limnol. Oceanogr. **62**: 2023–2044. doi:10.1002/lno.10549

Cortés, A., and S. MacIntyre. 2020. Mixing processes in small arctic lakes during spring. Limnol. Oceanogr. **65**: 260–288. doi:10.1002/lno.11296

Daniels, W. C., G. W. Kling, and A. E. Giblin. 2015. Benthic community metabolism in deep and shallow Arctic lakes during 13 years of whole–lake fertilization. Limnol. Oceanogr. **60**: 1604–1618. doi:10.1002/lno.10120

Del Giorgio, P., and P. Williams. 2005. Respiration in aquatic ecosystems. OUP Oxford.

Denfeld, B. A., H. M. Baulch, P. A. del Giorgio, S. E. Hampton, and J. Karlsson. 2018. A synthesis of carbon dioxide and methane dynamics during the ice-covered period of northern lakes. Limnol. Oceanogr. Lett. **3**: 117–131. doi:10.1002/lol2.10079

Ducharme-Riel, V., D. Vachon, P. A. del Giorgio, and Y. T. Prairie. 2015. The relative contribution of winter under-ice and summer hypolimnetic CO2 accumulation to the annual CO2 rmissions from northern lakes. Ecosystems **18**: 547–559. doi:10.1007/s10021-015-9846-0

Ellis, C. R., and H. G. Stefan. 1989. Oxygen demand in ice covered lakes as it pertains to winter aeration. J. Am. Water Resour. Assoc. **25**: 1169–1176. doi:10.1111/j.1752-1688.1989.tb01329.x

Evans, M. A., S. MacIntyre, and G. W. Kling. 2008. Internal wave effects on primary productivity: Experiments, theory and modeling. Limnol. Oceanogr. **53**: 339–353.

Farmer, D. M. 1975. Penetrative convection in the absence of mean shear. Q. J. R. Meteorol. Soc. **101**: 869–891. doi:10.1002/qj.49710143011

Giblin, A., and G. Kling. 2022. Chlorophyll a and primary productivity data for various lakes near Toolik Research Station. Arctic LTER. Summer 2010 to 2020. doi:10.6073/PASTA/1981B68E5B34E2A87436CDF76E40B417

Golosov, S., O. A. Maher, E. Schipunova, A. Terzhevik, G. Zdorovennova, and G. Kirillin. 2007. Physical background of the development of oxygen depletion in ice-covered lakes. Oecologia **151**: 331–340. doi:10.1007/s00442-006-0543-8

Gudasz, C., D. Bastviken, K. Steger, K. Premke, S. Sobek, and L. J. Tranvik. 2010. Temperature-controlled organic carbon mineralization in lake sediments. Nature **466**: 478–481. doi:10.1038/nature09186

Hawes, I., and A.-M. Schwarz. 1999. Photosynthesis in an extreme shade environment: Benthic microbial Mats from Lake Hoare, a permanently ice-covered Antarctic lake. J. Phycol. **35**: 448–459. doi:10.1046/j.1529-8817.1999.3530448.x

Hazuková, V., B. T. Burpee, I. McFarlane-Wilson, and J. E. Saros. 2021. Under ice and early summer phytoplankton dynamics in two Arctic Lakes with differing DOC. J. Geophys. Res. Biogeosci. **126**: e2020JG005972. doi:10.1029/2020JG005972

Hecky, R. E., and R. H. Hesslein. 1995. Contributions of benthic algae to Lake food webs as revealed by stable isotope analysis. J. North Am. Benthol. Soc. **14**: 631–653. doi:10.2307/1467546

Hrycik, A. R., and J. D. Stockwell. 2021. Under-ice mesocosms reveal the primacy of light but the importance of zooplankton in winter phytoplankton dynamics. Limnol. Oceanogr. **66**: 481–495. doi:10.1002/lno.11618

Huang, W., Z. Zhang, Z. Li, M. Leppäranta, L. Arvola, S. Song, J. Huotari, and Z. Lin. 2021. Under-ice dissolved oxygen and metabolism dynamics in a shallow Lake: The critical role of ice and snow. Water Resour. Res. **57**: e2020WR027990. doi:10.1029/2020WR027990

Hudson, J. M., A. B. Michaud, D. Emerson, and Y.-P. Chin. 2022. Spatial distribution and biogeochemistry of redox active species in arctic sedimentary porewaters and seeps. Environ. Sci. Process. Impacts **24**: 426–438. doi:10.1039/D1EM00505G

Jansen, J., B. F. Thornton, M. M. Jammet, M. Wik, A. Cortés, T. Friborg, S. MacIntyre, and P. M. Crill. 2019. Climate-sensitive controls on large spring emissions of CH4 and CO2 from Northern Lakes. J. Geophys. Res. Biogeosci **124**: 2379–2399. doi:10.1029/2019JG005094

Jansen, J., and others. 2021. Winter limnology: How do hydrodynamics and biogeochemistry shape ecosystems under ice. J. Geophys. Res. Biogeosci **126**: e2020JG006237.

Jewson, D. H., N. G. Granin, A. A. Zhdanov, and R. Y. Gnatovsky. 2009. Effect of snow depth on under-ice irradiance and growth of Aulacoseira baicalensis in Lake Baikal. Aquat. Ecol. **43**: 673–679. doi:10.1007/s10452-009-9267-2

Karlsson, J., J. Ask, and M. Jansson. 2008. Winter respiration of allochthonous and autochthonous organic carbon in a subarctic clear-water lake. Limnol. Oceanogr. **53**: 948–954. doi:10.4319/lo.2008.53.3.0948

Karlsson, J., and others. 2010. Quantifying the relative importance of lake emissions in the carbon budget of a subarctic catchment. J. Geophys. Res. Biogeosci **115**: G03006. doi:10.1029/2010JG001305

Karlsson, J., R. Giesler, J. Persson, and E. Lundin. 2013. High emission of carbon dioxide and methane during ice thaw in high latitude lakes. Geophys. Res. Lett. **40**: 1123–1127. doi:10.1002/grl.50152

Kirillin, G., C. Engelhardt, S. Golosov, and T. Hintze. 2009. Basin-scale internal waves in the bottom boundary layer of ice-covered Lake Müggelsee Germany. Aquat. Ecol. **43**: 641–651. doi:10.1007/s10452-009-9274-3

Kirillin, G., and others. 2012. Physics of seasonally ice-covered lakes: A review. Aquat. Sci. **74**: 659–682. doi:10.1007/s00027-012-0279-y

Kling, G. W., G. W. Kipphut, M. M. Miller, and W. J. O'Brien. 2000. Integration of lakes and streams in a landscape perspective: The importance of material processing on spatial patterns and temporal coherence. Freshw. Biol. **43**: 477–497.

Kremer, C. T., M. K. Thomas, and E. Litchman. 2017. Temperature- and size-scaling of phytoplankton population growth rates: Reconciling the Eppley curve and the metabolic theory of ecology. Limnol. Oceanogr. **62**: 1658–1670. doi:10.1002/lno.10523

Leppi, J. C., C. D. Arp, and M. S. Whitman. 2016. Predicting late winter dissolved oxygen levels in arctic lakes using morphology and landscape metrics. Environ. Manage. **57**: 463–473. doi:10.1007/s00267-015-0622-x

Livingstone, D. M., and D. M. Imboden. 1996. The prediction of hypolimnetic oxygen profiles: A plea for a deductive approach. Can. J. Fish. Aquat. Sci. **53**: 924–932. doi:10.1139/f95-230

Lizotte, M. P. 2008. Phytoplankton and primary production. *In* W. F. Vincent and J. Laybourne-Parry [eds.], Polar lakes and rivers: Limnology of Arctic and Antarctic aquatic ecosystems. Oxford University Press, p. 157–178.

Lorke, A., B. Müller, M. Maerki, and A. Wüest. 2003. Breathing sediments: The control of diffusive transport across the sediment: Water interface by periodic boundary-layer turbulence. Limnol. Oceanogr. **48**: 2077–2085. doi:10.2307/3597808

Luecke, C., and others. 2014. Alaska's changing Arctic: Ecological consequences for tundra, streams, and lakes. Oxford University Press, p. 238–286.

MacIntyre, S., J. P. Fram, P. J. Kushner, N. D. Bettez, W. J. O'Brien, J. E. Hobbie, and G. W. Kling. 2009. Climate-related variations in mixing dynamics in an Alaskan arctic lake. Limnol. Oceanogr. **54**: 2401–2417. doi:10.4319/lo.2009.54.6_part_2.2401

MacIntyre, S., R. Wanninkhof, and J. P. Chanton. 1995. Biogenic trace gases: Measuring emissions from soil and water. Blackwell, p. 52–97.

MacIntyre, S., A. Cortés, and S. Sadro. 2018. Sediment respiration drives circulation and production of CO2 in ice-covered Alaskan arctic lakes. Limnol. Oceanogr. Lett. **3**: 302–310. doi:10.1002/lol2.10083

Malm, J. 1998. Bottom buoyancy layer in an ice-covered lake. Water Resour. Res. **34**: 2981–2993. doi:10.1029/98WR01904

Michaud, A. B., and S. Apollonio. 2022. Overwinter oxygen and silicate dynamics in a high Arctic Lake (Immerk Lake, Devon Island, Canada). Inland Waters **0**: 1–9. doi:10.1080/20442041.2022.2063623

Mortimer, C. H., and F. J. Mackereth. 1958. Convection and consequences in ice covered lakes. Verh Intern. Ver. Limnol **13**: 923–932. doi:10.1080/03680770.1956.11895490

Müller, B., L. D. Bryant, A. Matzinger, and A. Wüest. 2012. Hypolimnetic oxygen depletion in eutrophic lakes. Environ. Sci. Technol. **46**: 9964–9971. doi:10.1021/es301422r

Obertegger, U. 2022. Temporal and spatial differences of the under-ice microbiome are linked to light transparency and chlorophyll-a. Hydrobiologia **849**: 1593–1612.

O'Brien, W. J., M. Barfield, N. Bettez, A. E. Hershey, J. E. Hobbie, G. Kipphut, G. Kling, and M. C. Miller. 2005. Long-term response and recovery to nutrient addition of a partitioned arctic lake. Freshw. Biol. **50**: 731–741. doi:10.1111/j.1365-2427.2005.01354.x

Petrov, M. P., A. Y. Terzhevik, R. E. Zdorovennov, and G. E. Zdorovennova. 2006. The thermal structure of a shallow lake in early winter. Water Resour. **33**: 135–143. doi:10.1134/S0097807806020035

Petrov, M. P., A. Y. Terzhevik, R. E. Zdorovennov, and G. E. Zdorovennova. 2007. Motion of water in an ice-covered shallow lake. Water Resour. **34**: 113–122. doi:10.1134/S0097807807020017

Pulkkanen, M., and K. Salonen. 2013. Accumulation of low oxygen water in deep waters of ice-covered lakes cooled below 4 °C. Inland Waters **3**: 15–24. doi:10.5268/IW-3.1.514

Rizk, W., G. Kirillin, and M. Leppäranta. 2014. Basin-scale circulation and heat fluxes in ice-covered lakes. Limnol. Oceanogr. **59**: 445–464.

Sadro, S., C. E. Nelson, and J. M. Melack. 2011. Linking diel patterns in community respiration to bacterioplankton in an oligotrophic high-elevation lake. Limnol. Oceanogr. **56**: 540–550. doi:10.4319/lo.2011.56.2.0540

Scholander, P. F., W. Flagg, R. J. Hock, and L. Irving. 1953. Studies on the physiology of frozen plants and animals in the arctic. J. Cell. Comp. Physiol. **42**: 1–56. doi:10.1002/jcp.1030420403

Schwefel, R., M. Hondzo, A. Wüest, and D. Bouffard. 2017. Scaling oxygen microprofiles at the sediment interface of deep stratified waters. Geophys. Res. Lett. **44**: 1340–1349. doi:10.1002/2016GL072079

Seekell, D. A., J.-F. Lapierre, J. Ask, A.-K. Bergström, A. Deininger, P. Rodríguez, and J. Karlsson. 2015. The influence of dissolved organic carbon on primary production in northern lakes. Limnol. Oceanogr. **60**: 1276–1285. doi:10.1002/lno.10096

Smits, A. P., N. W. Gomez, J. Dozier, and S. Sadro. 2021. Winter climate and Lake morphology control ice phenology and under-ice temperature and oxygen regimes in Mountain Lakes. J. Geophys. Res. Biogeosciences **126**: e2021JG006277. doi:10.1029/2021JG006277

Sturm, M., and G. E. Liston. 2003. The snow cover on lakes of the Arctic coastal plain of Alaska USA. J. Glaciol. **49**: 370–380.

Terzhevik, A., and others. 2009. Some features of the thermal and dissolved oxygen structure in boreal, shallow ice-covered Lake Vendyurskoe. Russia. Aquat. Ecol. **43**: 617–627. doi:10.1007/s10452-009-9288-x

Terzhevik, A. Y., and others. 2010. Hydrophysical aspects of oxygen regime formation in a shallow ice-covered lake. Water Resour. **37**: 662–673. doi:10.1134/S0097807810050064

Vincent, W. F., R. W. Castenholz, M. T. Downes, and C. Howard-Williams. 1993. Antarctic cyanobacteria: Light, nutrients, and photosynthesis in the microbial mat Environment1. J. Phycol. **29**: 745–755. doi:10.1111/j.0022-3646.1993.00745.x

Whalen, S. C., and V. Alexander. 1986. Seasonal inorganic carbon and nitrogen transport by phytoplankton in an Arctic Lake. Can. J. Fish. Aquat. Sci. **43**: 1177–1186. doi:10.1139/f86-147

Whalen, S. C., B. A. Chalfant, and E. N. Fischer. 2008. Epipelic and pelagic primary production in Alaskan Arctic lakes of varying depth. Hydrobiologia. **614**: 243–257. doi:10.1007/s10750-008-9510-1

Wüest, A., and A. Lorke. 2003. Small-scale hydrodynamics in lakes. Annu. Rev. Fluid Mech. **35**: 373–412. doi:10.1146/annurev.fluid.35.101101.161220

Zdorovennova, G., N. Palshin, R. Zdorovennov, S. Golosov, T. Efremova, G. Gavrilenko, and A. Terzhevik. 2016. The oxygen regime of a shallow lake. Geogr. Environ. Sustain. **9**: 47–57. doi:10.15356/2071-9388_02v09_2016_04

Acknowledgments

Conflict of interest

The authors declare that there is no conflict of interest regarding the publication of this article.